Coordination Chemistry Reviews
Elsevier Publishing Company, Amsterdam – Printed in The Netherlands

MANGANESE PORPHYRIN COMPLEXES

L.J. BOUCHER

Department of Chemistry, Carnegie-Mellon University, Pittsburgh, Pennsylvania 15213 (U.S.A.)

(Received May 5th, 1971)

CONTENTS

A. INTRODUCTION

There is a growing interest in metalloporphyrins among inorganic chemists because of the unique nature of the coordination chemistry of these materials [1] and also because of their obvious relevance as biological models [2]. Although a large number of metalloporphyrins have been examined, most of the detailed work has involved the iron porphyrins [3]. Surprisingly, a sizable body of literature also now exists for the analogous manganese complexes. Manganese porphyrins are of considerable interest for several reasons. For one, the unique absorption spectrum of the Mn^{III} complexes is presumably diagnostic of an unusual electronic structure [4]. A thorough understanding of Mn porphyrins would be valuable in sorting out the closely related and biologically important Fe system, as well as for the general understanding of metalloporphyrin spectra and structure. A second reason is the utility of the porphyrin complexes as model compounds

in the study of the manganese-dependent oxygen evolution in green-plant photosynthesis[5,6]. Because of the increasing activity in this area, it seems appropriate to review the coordination chemistry of Mn porphyrins. This review attempts to present the information about Mn porphyrin complexes and, by interpreting this data, to propose electronic and molecular structures as well as reactivity patterns for the complexes. The biological implications of these results will then be discussed in relation to the Fe porphyrins and the role of manganese in photosynthesis. Although the discussion will be generally restricted to Mn porphyrins, reference is made to other metalloporphyrin systems when appropriate. It is hoped that the gaps in our understanding of Mn porphyrins uncovered here will stimulate others to undertake the needed research.

Although a manganese porphyrin complex was first reported by Zaleski [7] in 1904, it was not until 50 years later that Calvin [8] and co-workers published a series of papers relating the preparation and properties of these materials. For coordination compounds the most common oxidation states of manganese are Mn^{II}, Mn^{III} and Mn^{IV} (see ref. 9). Although all these oxidation states appear to be accessible to the porphyrin complexes [8], the stable complexes [10] are those of Mn^{III}. The lower and higher oxidation states can then be generated by the appropriate reduction and oxidation of Mn^{III} porphyrins. Because most of the work reported to date has concerned Mn^{III} porphyrins, these will be

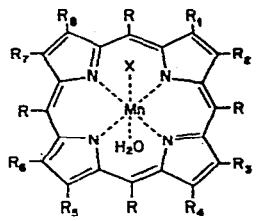

Compound		Substituents [a]								
		R	R_1	R_2	R_3	R_4	R_5	R_6	R_7	R_8
Deuteroporphyrin IX dimethylester	DMDepor	H	M	H	M	H	M	PrM	PrM	M
Deuteroporphyrin IX	DePor	H	M	H	M	H	M	PrH	PrH	M
Mesoporphyrin IX dimethylester	DMMesopor	H	M	E	M	E	M	PrM	PrM	M
Mesoporphyrin IX	Mesopor	H	M	E	M	E	M	PrH	PrH	M
Hematoporphyrin IX dimethylester	DMHpor	H	M	ME	M	ME	M	PrM	PrM	M
Hematoporphyrin IX	Hpor	H	M	ME	M	ME	M	PrH	PrH	M
Protoporphyrin IX dimethylester	DMPrpor	H	M	V	M	V	M	PrM	PrM	M
Protoporphyrin IX	Prpor	H	M	V	M	V	M	PrH	PrH	M
Etioporphyrin I	Etio	H	M	E	M	E	M	E	M	E
Octaethylporphyrin	OEP	H	E	E	E	E	E	E	E	E
Tetraphenylporphine	TPP	Ph	H	H	H	H	H	H	H	H
Tetrapyridylporphine	TPPy	Py	H	H	H	H	H	H	H	H
Porphine	Porp	H	H	H	H	H	H	H	H	H

[a] M = CH_3; E = CH_2CH_3; V = $CH{=}CH_2$; ME = $CHOHCH_3$; PrM = $CH_2CH_2CO_2CH_3$; PrH = $CH_2CH_2CO_2H$; Ph = C_6H_5; Py = NC_5H_4.

Fig. 1. Structural representation of Mn^{III} porphyrin complexes.

discussed first. A discussion of Mn^{II} and Mn^{IV} porphyrins as well as of the closely related chlorophyll and phthalocyanine derivatives follows. Structural representations of the commonly used porphyrins and the abbreviations used throughout this review are given in Fig. 1.

B. MANGANESE(III) PORPHYRINS

(i) Synthesis

When excess Mn^{II} acetate and porphyrin (H_2Por) are refluxed in glacial acetic acid (or dimethylformamide [11]) in the presence of air, the acetate salt of the Mn^{III} porphyrin is readily formed [4,12]. The reaction appears to proceed in two distinct steps [13].

$$Mn^{2+} + H_2Por \underset{k_{-1}}{\overset{k_1}{\rightleftharpoons}} [Mn(Por)] + 2H^+ \quad (1)$$

$$[Mn(Por)] \xrightarrow{[O_2]} [Mn(Por)]^+ \quad (2)$$

The first step is most likely rate-determining and the second step is very rapid and essentially irreversible. In glacial acetic acid, $k_{-1} \gg k_1$ and in the absence of oxygen the Mn^{2+} insertion does not proceed. Like most trivalent metal ions, Mn^{3+} insertion in the porphyrin is not noted [10]. The rate of insertion in glacial acetic acid is second-order overall, first-order in metal ion and first-order in porphyrin. For Hpor, the activation energy is 16.4 kcal/mole and the activation entropy is -12 cal deg^{-1} $mole^{-1}$ (ref. 14). Addition of 1% H_2O to the glacial acetic acid altered the activation energy to 15.7 kcal/mole and the activation entropy to -16 cal deg^{-1} $mole^{-1}$. A somewhat higher activation energy, 18.7 kcal/mole, has been determined for the insertion of Mn^{2+} into TPPy in glacial acetic acid [15] Unfortunately, no kinetic data have been obtained for Mn^{2+} insertion reactions under physiological conditions, i.e., pH 7 aqueous solution. The mechanism for metal insertion most likely involves a rapid pre-equilibrium to form an $Mn^{2+} \cdot H_3Por^+$ intermediate and this is followed by a slow insertion reaction. The activation step is probably dissociative and may involve a multiple desolvation of the metal ion [16] which is required by the semi-rigid nature of the porphyrin for metal binding. This effect is most likely responsible for the fact that Mn^{2+} reacts more slowly with porphyrins (by a factor of $> 10^6$) than it does with simple bidentate ligands [17].

The acetate ion of the Mn^{III} porphyrin complex can be replaced by another anion by dissolution in water and subsequent addition of a large excess of the sodium salt of the appropriate anion. This results in the rapid precipitation of the desired complex [4]

$$[Mn(Por)]^+ + X^- \rightarrow [Mn(Por)(X)H_2O] \quad (3)$$

where $X^- = F^-, Cl^-, Br^-, I^-, SCN^-, N_3^-, CNO^-, NO_2^-$. The ions SO_4^{2-} and PO_4^{3-} do not yield a product. Surprisingly, the cyanide ion does not form a complex. In fact, the product that precipitates out of 1 *M* sodium cyanide in aqueous solution at pH 4 to 7 is the hydroxide complex [18]. Also, salts of the dianion complexes are not formed. In general, the best

method of purification of the complexes is reprecipitation from aqueous solution. Thin-layer chromatography and elemental analyses prove to be satisfactory criteria of purity. From elemental analyses, the materials appear to have the composition $Mn(Por)(X)H_2O$. Attempts to prepare other solvates by replacing the coordinated water with pyridine, methanol or dimethylsulfoxide by precipitation of the complexes out of these solvents have been unsuccessful [18]. Further, drying at 110° in vacuo over P_2O_5 does not remove the water. The question as to whether the water is coordinated to the metal and the related question of the coordination number in the solid state for Mn^{III} porphyrins remain open. Mn^{III} complexes of all the anions above have been prepared with DMPrpor and Etio [4,19]. It should be quite easy to prepare similar complexes of all the porphyrins given in Fig. 1; indeed, the Cl^- complex of all of these has been synthesized [19]. In addition, the following materials have been reported: $[Mn(Por)(OH)H_2O]$, Por = TPPy [20], Mesopor [12], DMMesopor [11], Hpor [21], Prpor [11], TPP [11], Depor [24]; $[Mn(Por)(C_2H_3O_2)H_2O]$, por = Hpor [21], OEP [22], DMMesopor [23], Etio [25]; $[Mn(Etio)(C_2H_3O_3)C_2H_4O_2]$ [26]; $[Mn(Por)(Cl)H_2O]$, Por = OEP [22], Hpor [27], Mesopor [27]. In those instances where multiple reports exist, reference to only one paper is made. In most cases the presence of the coordinated water is assumed, even where elemental analyses are not presented. Otherwise, the formulations given correspond to those of the original workers. It must be pointed out that elemental analyses given for the acetate salts can equally well be fit by assuming a hydroxy(aquo) complex. It seems a general observation that the only species that is isolated from aqueous solution in the absence of a large excess of coordinating anion is the hydroxide complex. As a result, this appears as a common impurity in the preparation of the other anion complexes. Further column chromatography of the anion complexes on silica gel or alumina also yields the hydroxide complex [18].

(ii) Axial ligation

When Mn^{III} porphyrins are dissolved in a coordinating solvent like pyridine, methanol or dimethylsulfoxide, axial ligands are displaced by the solvent molecules.

$$[Mn(Por)(X)H_2O] + B \leftrightarrows [Mn(Por)(X)B] + H_2O \qquad K_1 \qquad (4)$$

$$[Mn(Por)(X)B] + B \rightleftarrows [Mn(Por)B_2]^+ + X^- \qquad K_2 \qquad (5)$$

The observation that the absorption spectra of these solutions are independent of the anion in the starting material for all the anion complexes indicates that the same species, the solvent complex, is present in all the solutions [4]. If limited amounts of the donor molecule are used in an inert solvent, then the binding constants can be determined spectrophotometrically. Measurements of K_1 for pyridine (Py) binding [27] in chloroform at 25°C have been made for $[Mn(Por)(Cl)H_2O]$ where por = TPP, Mesopor and Hpor. The $\log K_1$ values are 0.40, 0.54 and 0.34, respectively. The order Mesopor > TPP > Hpor does not follow the donor ability of the porphyrin. It must be pointed out, however, that K_1 varies by less than a factor of 2 here and is therefore rather insensitive to the porphyrin. Values of K_2 were not reported. The pyridine binding constants for $[Mn(Mesopor(OH)H_2O]$ have been determined in aqueous solution by a combination of spectrophotometric and

potentiometric methods [12]. The data are consistent with the binding of two pyridine molecules per monomeric complex. It was found that $K_1 = 5.9 \times 10^{-2}$ and $K_2 = 1.9$ at 30°C. The values are independent of pH in the 7–12 range. Reaction of solid [Mn(Etio)$(C_2H_3O_2)H_2O$] with excess pyridine vapor results in the binding of a molecule of pyridine at room temperature in vacuo [25]. This is only slowly lost at ~150°C in vacuo. The binding of pyridine probably involves replacing the axially coordinated water.

The pK_a for the reaction in aqueous solution at 22.5°C was found to be 11.95 by spectrophotometric and potentiometric techniques [10].

$$[Mn(Prpor)(H_2O)_2]^+ \rightleftarrows [Mn(Prpor)(OH)H_2O] + H^+ \quad (6)$$

The corresponding pK_a value for [Mn(DMPrpor)(OH)H_2O] is 11.3. Dilute solutions were used to avoid problems arising from metalloporphyrin aggregation. The formation of a dihydroxo complex is not noted even at pH 14. In addition to the formation of the hydroxide complex at high pH in aqueous solution, there is the possibility for a slow dimerization reaction

$$2[MnPor(OH)H_2O] \rightleftarrows [(H_2O)PorMn{-}O{-}MnPor(H_2O)] + H_2O \quad (7)$$

Although the existence of such a dimer for [Mn(TPP)(OH)H_2O] has been alluded to in a recent review article, the preparation and characterization of the material have not been reported [28]. (see Note added in proof, p. 327).

Equilibrium constants have also been measured for the formation of charge transfer complexes for a number of acceptors and donors and [Mn(DMMesopor)(OH)H_2O] in methylene chloride at 25°C [29]. Fairly stable complexes are formed with acceptors like trinitrofluorenone ($K = 250\,M^{-1}$) and trinitrobenzene ($K = 30\,M^{-1}$). Conversely, donor molecules like the oxygen-containing *p*-dimethoxybenzene ($K = 0.2\,M^{-1}$), the nitrogen-containing *N,N*-dimethylaniline ($K \sim 1\,M^{-1}$) and the hydrocarbon, hexamethylbenzene ($K = 2.5\,M^{-1}$) form weak complexes. Interestingly, steroid donors, like cholestanone ($K = 40\,M^{-1}$), cholestene ($K = 75\,M^{-1}$) and cholestanol ($K = 250\,M^{-1}$) give stable adducts. As with most metalloporphyrins, Mn^{III} porphyrins are better charge-transfer donors than acceptors; i.e. the porphyrin π cloud interacts strongly with acceptor molecules but not with donor molecules. No simple correlation between the stability constants and any parameters of the acceptors or donors which could be associated with so-called charge-transfer forces exists. The strong binding of the steroid molecules may be related to their large size or to the possibility of these molecules binding to the metal atoms in the axial positions. The latter seems unlikely since the equilibrium constants are several orders of magnitude larger for steroid binding than for axial pyridine binding. This points up the relative importance of porphyrin interaction vis-a-vis metal interactions.

In addition to the scattered thermodynamic studies on axial ligation, only one report appears in the literature of the kinetic parameters for this process. Solvent exchange kinetics have been measured by proton NMR line broadening for both methanol and dimethylformamide solvated [Mn(DMPrpor)]$^+$ (ref. 30). In methanol, the activation parameters are $\Delta H^{\ddagger} = 8.0 \pm 0.3$ kcal/mole and $\Delta S^{\ddagger} = 1.3 \pm 1.5$ cal.mole^{-1}.deg^{-1}, giving a first-order rate constant for exchange at 25° of 1.5×10^7 sec^{-1}. In dimethylformamide, the

activation parameters are $\Delta H^{\ddagger} = 10.5$ kcal/mole, $\Delta S^{\ddagger} = 12.4$ cal.mole^{-1}.deg^{-1}, giving a rate constant for exchange at 25°C of 6.4×10^7 sec^{-1}. It is readily seen that axial ligation is extremely rapid and that the rate is sensitive to the ligand. The rate-determining step in these reactions is thought to be a dissociation of the axially bound solvent molecule in the complex, like $[Mn(DMPrpor)(CH_3OH)_2]^+$. Kinetic measurements on anation reactions of $[Mn(Hpor)(OH)H_2O]$ in aqueous solution at pH 7.2 were attempted with N_3^-, SCN^- and CN^-. No complex formation could be noted spectrophotometrically at 0.15 *M* anion for 2×10^{-5} *M* solution of the complex. Since axial ligation appears to be a rapid reaction, the failure to observe anation must be related to a highly unfavorable stability constant for the binding of N_3^-, SCN^- or CN^-. Finally, the kinetics of anion exchange have not been measured.

It is obvious that much more information about axial binding in Mn^{III} porphyrins is needed before any detailed discussion can be initiated. However, there are several points that can be made with the data at hand. For one, it appears that the two axial ligands are not bound equally strongly. For example, the addition of a second pyridine molecule to $[Mn(Mesopor)(OH)H_2O]$ is favored over the addition of the first by a factor of ~30. The addition of the first pyridine molecule is assumed to lead to binding of the donor in the axial position *trans* to the hydroxide ion. It is interesting to note that the rather small equilibrium constant for this process is about equal to that for pyridine binding to [Mg(Por)Py] [32]. Surprisingly, the replacement of the axially coordinated hydroxide ion appears to be slightly enhanced in [Mn(Mesopor)OHPy]. This appears not to be the case in the corresponding Fe^{III} system. This latter case, however, is complicated by the formation of dimeric species [33]. Since the axial ligations probably involve replacement reactions, it is difficult to say in an absolute sense whether axial ligation is weak or strong. It could be that the manganese atom prefers binding to oxygen donors like hydroxide and water over the nitrogen donor pyridine. More detailed measurements with a variety of donors and anion complexes would help to settle this point. When Mn^{III} porphyrins are dissolved in coordinating solvents, the two axial ligands are now the same. A question which remains to be answered is whether the two axial ligands are equivalent thermodynamically and kinetically.

(iii) Spectroscopy

A wide variety of spectroscopic techniques can be used not only to characterize Mn^{III} porphyrins but also to aid in sorting out problems relating to structure and bonding. Rock salt infrared spectra are useful in showing that the integrity of the porphyrin skeleton and peripheral substituents are maintained during the formation of the complex [4]. Anion-dependent IR absorptions, ν(Mn–Cl) = 260–280 cm^{-1} (ref. 34), ν(MnBr) ~ 210 cm^{-1}, ν(Mn–I) ~ 190 cm^{-1} and ν(Mn–F) ~ 460 cm^{-1} are also seen [4]. The IR spectra are consistent with the notion that the anions are axially bound to the manganese in the solid state. Whether or not a water molecule is coordinately bound is somewhat more difficult to assess. The solid state and chloroform solution spectra do, however, show prominent absorption at 3450 cm^{-1} and 1620 cm^{-1} which might be assigned to coordinated water vibrations [4]. For anions like N_3^-, NCO^- and SCN^-, multiple bond stretching absorption is seen, e.g. $\nu(N_3^-) = 2020$ cm^{-1}, $\nu(NCO^-) = 2175$ cm^{-1} and $\nu(SCN^-) = 2050$ cm^{-1}. The NO_2^- complex shows the $\nu_s(NO_2^-)$ absorption at 1275 cm^{-1}. In general, the frequencies

TABLE 1

Magnetic moments for manganese porphyrins

Complex	Condition [a]	μ_{eff} (B.M.)	Ref.
Mn^{III}			
[Mn(DMHpor)(Cl)H_2O]	Solid	4.7	10
	Aqueous solution, pH 7	4.9	10
[Mn(Hpor)(OH)H_2O]	Solid	4.8	10
	Aqueous solution, pH 11	4.9	10
	20% Pyridine–water, pH 11	4.9	10
[Mn(Hpor)(Cl)H_2O]	Solid	4.88	37
[Mn(DMPrpor)(Cl)H_2O]	Solid	4.79	4
	Methanol solution	5.01	30
[Mn(DMPrpor)(Br)H_2O]	Solid	4.87	4
[Mn(DMPrpor)(I)H_2O]	Solid	4.86	4
[Mn(DMPrpor)(F)H_2O	Solid	4.92	4
[Mn(DMPrpor)(CNO)H_2O]	Solid	4.89	18
[Mn(DMPrpor)(SCN)H_2O]	Solid	4.63	18
[Mn(DMPrpor)(OH)H_2O]	Solid	4.83	18
[Mn(DMPrpor)(N_3)H_2O]	Solid	4.89	18
[Mn(DMPrpor)($C_2H_3O_2$)H_2O	Solid	4.86	18
[Mn(DMHpor)(Cl)H_2O]	Solid	4.69	18
[Mn(DMMesopor)(Cl)H_2O]	Solid	4.92	18
[Mn(DMMesopor)(Cl)H_2O]	Solid	3.4	38
[Mn(DMDepor)(Cl)H_2O]	Solid	4.79	18
[Mn(Etio)(Cl)H_2O	Solid	4.79	18
[Mn(TPP)(Cl)H_2O]	Solid	4.89	18
	10% Water–pyridine	4.76	18
[Mn(TPP)(OH)H_2O]	Solid	4.93	18
[Mn(Mepheo$_a$)(Cl)H_2O]	Solid	4.76	9
Mn^{II}			
[Mn(Hpor)H_2O]	Aqueous solution, pH 13	5.8	10
	20% Pyridine–water, pH 13	5.9	10
[Mn(Mesopor)H_2O]	Solid	2.82	39
	Solid	3.04	39
	Pyridine	2.88	39
	Pyridine–water	2.69	39
[Mn(Prpor)H_2O]	Solid	3.86	39
Mn^{IV}			
[Mn(Hpor)$(OH)_2$]	Aqueous solution, pH 13	2.0	10

[a] Temperature 20–25°C.

are close to the free ion values and appear to be consistent with N-bonded pseudo-halides [35]. A more detailed look at the solution infrared spectra, in both the high- and low-frequency regions of the different Mn^{III} porphyrin anion complexes, may lead to valuable information about the axial binding of the anions [36].

The oxidation state of Mn^{III} porphyrins has been confirmed by magnetic susceptibility measurements of the complexes in the solid state [4,34]. Some of the reported data are given in Table 1. The magnetic moments are generally in the 4.8–5.0 B.M. range, values entirely consistent with a high-spin d^4 case, i.e. Mn^{III}. Room-temperature solution measurements in pyridine–water also give magnetic moments of 4.8–5.0 B.M. In the case of solid [Mn(Hpor)(Cl)H_2O], variable temperature (80–300°K) magnetic susceptibility measurements have been made [10,37]. Similar measurements have also been made for [Mn(DMPrpor)(Cl)H_2O] in methanol, 213–313°K. The data adhere to the Curie law with a Weiss constant of approximately zero [10,30,37]. Early measurements yielded magnetic moments for solid [Mn(Mesopor)(Cl)H_2O] of 3.4 B.M. [38]. More recently, [Mn(TPP)(OH)H_2O] has been found to have a magnetic moment of 4.9 B.M. These observations may be rationalized if the materials examined actually contain variable amounts of a spin-paired oxo-bridged dimer. A detailed thermomagnetic analysis of Mn^{III} porphyrin complexes would now be useful in obtaining the ground-state term and zero-field splittings of these materials [40].

Magnetic resonance techniques have been little applied to the study of Mn^{III} porphyrins. No attributable ESR absorption has been observed at −196°C for [Mn(Por)(OH)H_2O] (Por = Prpor, Mesopor, Depor, Hpor) in water [24]. This occurs because high-spin d^4 complexes have an even number of spins which can result in a singlet ground state (not a Kramer's doublet) with a large zero-field splitting. The zero-field splitting of [Mn(DMDepor)(Cl)H_2O] has been determined to be 7.6 cm^{-1} by direct infrared measurement [41]. Electron spin relaxation of Mn^{III} is rapid at room temperature. The latter fact is exploited in measuring proton magnetic resonance spectra of the Mn^{III} complexes [42]. These contact shift measurements for Mn^{III} porphyrins can ultimately give the mode of spin delocalization in the complex which can be related to metal–ligand binding. Chemical shift measurements for [Mn(DMPrpor)(Cl)H_2O] gave hyperfine coupling constants for the axially bound solvent molecules for methanol hydroxy and methyl protons of 3.96×10^6 rad.sec^{-1} and 2.09×10^6 rad.sec^{-1}, respectively, and for dimethylformamide CH and methyl protons of 8.11×10^5 rad.sec^{-1} and 5.25×10^5 rad.sec^{-1}, respectively [30].

The most useful spectroscopic technique for the study of metalloporphyrins continues to be electronic absorption spectroscopy. The normal metalloporphyrin spectrum shows an intense B (Soret) band at ~24 kK and two weaker Q (α, β) bands at ~18 kK. A typical spectrum of this sort (for Mn^{II}) can be seen in Fig. 2. The absorption arises from $\pi \rightarrow \pi^*$ transitions of the aromatic porphyrin ligand. The widely accepted model to fit this spectrum, the four-orbital model, treats the porphyrin as a cyclic polyene and emphasizes the transition between the two highest filled bonding molecular orbital levels, a_{1u}, a_{2u} and the lowest empty doubly degenerate antibonding molecular orbital level, e_g^* [43]. The allowed transitions, $a_{1u} \rightarrow e_g^*$, $a_{2u} \rightarrow e_g^*$, are assumed to be near degenerate in energy. As a consequence, the states undergo configuration interaction and give rise to new states. The resulting absorption spectrum shows a high-energy band B in which the transition dipoles add (high intensity) and a low-energy band Q in which the transition dipoles nearly cancel

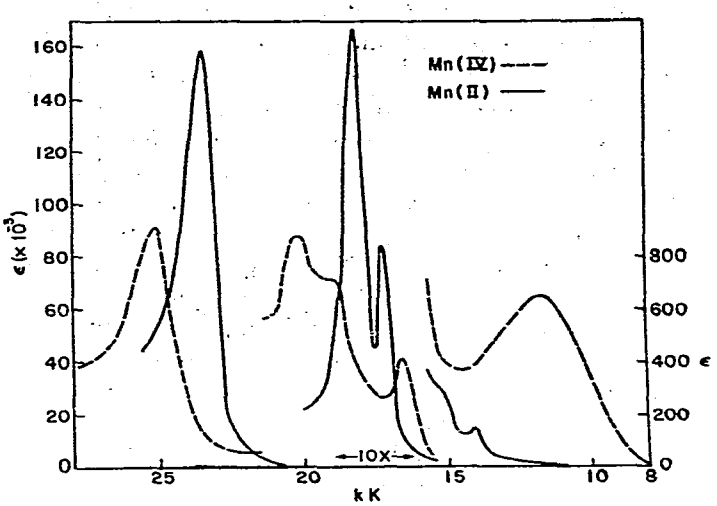

Fig. 2. Absorption spectra of chloro(aquo)mesoporphyrinIX dimethylestermanganese(III) in pyridine–water, pH 11, with $Na_2S_2O_4$ added (——) and in ethanol–water, pH 13, with NaOCl added (– – –).

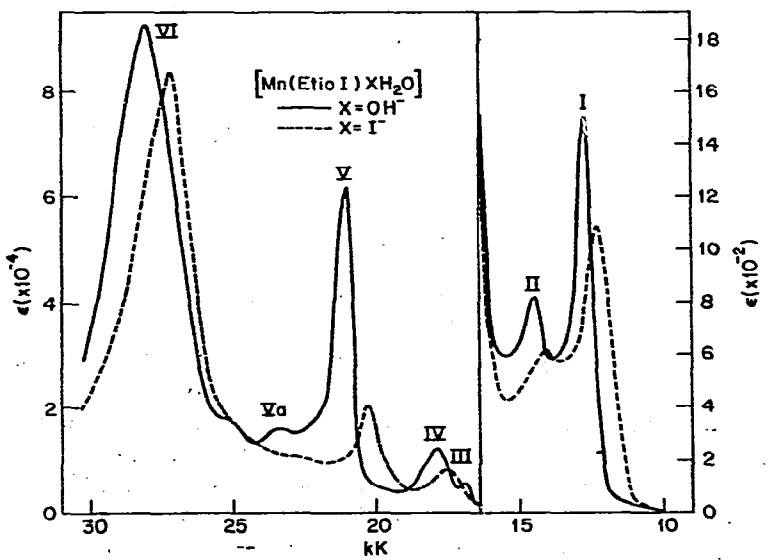

Fig. 3. Absorption spectra of anion(aquo)etioporphyrinI manganese(III) in chloroform.

(low intensity). The two Q bands are vibronic components of the same transition. The essential correctness of this model has been supported by the extensive molecular orbital calculations of Zerner and Gouterman [44]. The frequencies of the B and Q bands vary only slightly for a wide variety of metal ions [45] and exact positions of the maxima are related to a number of parameters including metal electronegativity and metalloporphyrin molecular structure, but not to the presence of metal d orbitals [46]. This is taken as evidence that the metal $d\pi$ orbitals and the porphyrin π orbitals are only weakly interacting.

Although the high-spin Fe^{III} porphyrins show anomalies, the most striking exceptions to the normal metalloporphyrin spectra are observed with the Mn^{III} porphyrins. A typical solution spectrum is given in Fig. 3. It is readily seen that while absorptions appear in the region of the Q band (bands III and IV) the B band is absent. Two high-intensity bands now appear in the 20–30 kK region (bands V and VI) along with two new low-intensity bands in the near infrared (bands I and II). An additional weak band, Va, is seen between bands V and VI. In most spectra, band III appears as a resolvable shoulder on the red side of band IV. Band VI is generally quite broad, indicating the presence of several overlapping absorptions. The anomalous spectrum would seem to indicate that Mn^{III} is strongly perturbing the porphyrin π system. This result has prompted the study of a number of the variables that might affect the frequencies of the absorption maxima. Work of this sort is not only useful in assigning the observed transitions but is also helpful in understanding any metal porphyrin interaction. In these spectral studies first the porphyrin was varied [34], then the coordinated anion [4,47], and then the solvent [29,47].

By changing the porphyrin β substituents, the pK_a of the ligand can be changed substantially; i.e. the donor strength of the porphyrin can be varied. The absorption spectra of a number of $[Mn(Por)(Cl)H_2O]$ complexes have been examined in chloroform and other solvents [34]. The frequencies of the absorption maxima are dependent on the particular porphyrin; the order is

$$\text{Porp} > \text{DMDepor} > \text{Etio} > \text{DMMesopor} > \text{DMHpor} > \text{DMprpor} > \text{TPPy} > \text{TPP} \qquad (8)$$

The order is also observed for $[Mn(Por)(OH)H_2O]$ in water (pH 7) where Por = Prpor Mesopor, Depor and Hpor [24]. For the fully β-substituted porphyrins, the order seems to follow donor ability, i.e. the stronger the porphyrin σ donor, the higher the energy of the transitions. All metalloporphyrin spectra presumably show this trend [48]. Electron-donating substituents place negative charge into the macrocycle and the porphyrin bonding and antibonding levels move apart. The relative position of Porp and DMDepor in the order must be related to the presence of hydrogen substituents in the β position of the porphyrin rather than to the donor strength of the porphyrin In a similar way, the position of TPP and TPPy may be related to the fact that they are the only meso substituted porphyrins in the order. The intensity of the absorptions vary with the porphyrin.[34]. In general, band VI is more intense than band V by a factor of 1.1–1.5. It is interesting to note that the porphine derivatives (Porp, TPP, TPPy) are the only derivatives which show the intensity of band V greater than band VI. The intensity ratio of band V to band VI increases in the sequence

$$\text{TPPy} > \text{TPP} > \text{Porp} > \text{DMPepor} > \text{DMHpor} > \text{DMPrpor} > \text{DMMesopor} > \text{Etio} \qquad (9)$$

It is readily seen that the highest members of the series are those porphyrins that have β-hydrogen substituents. A recent theoretical study of luminescent states in metalloporphyrins indicates that the porphyrin a_{2u} level is lower in energy than the a_{1u} level for the porphine ligands while the reverse is true for the fully β-substituted derivatives [49]. The observed energy and intensity orders (8 and 9) may be related to this. The effect of varying porphyrins on the Mn^{III} porphyrin spectrum is probably related more to the changes in the porphyrin π levels rather than to any great changes in the porphyrin–manganese interaction. This is supported by the observation that all the absorption bands, I–VI, shift in the same direction with change in β substituent. At any rate, the substituent shifts are not large; e.g. the spread is generally less than 1 kK for all the bands.

Spectral studies have been carried out with a number of anion complexes of [Mn(Etio)(X)H_2O] and [Mn(DMPrpor)(X)H_2O] [44]. For chloroform solutions, the frequencies of the absorption maxima are dependent on the axial anion. New data for [Mn(Etio)(X)H_2O] are collected in Table 2. The energy order for band V is

$$F^- > C_2H_3O_2^- > NCO^- > OH^- \sim Cl^- > N_3^- \sim NCS^- \sim Br^- > I^- \qquad (9)$$

Band V is most sensitive to the anion and the total spread is ~2.0 kK. All the other bands give a spread of from 0.6 to 1.0 kK. Within experimental error, the other bands give the same order as band V; i.e. no selective shifts are noted. The spectra of the [Mn(DMPrpor)(X)H_2O] complexes [47] also conform to this general pattern. The order $C_2H_3O_2^- > Cl^-$ is noted for [Mn(OEP)(X)H_2O] in methylene chloride [22]. [Mn(Hpor)(X)H_2O] shows the order $OH^- > H_2O$ (ref. 10). The intensity ratio of bands V/VI, R, also varies with the anion and roughly parallels the energy order, i.e. high energy, high ratio. The hard base character of the anion seems to offer an obvious correlation for the spectra [51]. Thus, it appears that hard base anions give absorption maxima at high energy while the soft base

TABLE 2

Absorption maxima of [Mn(Etio)(X)H_2O] in chloroform

Band	X^-									
	F	$C_2H_3O_2$	OH	Cl	NCO	N_3	NCS	NO_2	Br	I
I[a]	13.1	12.9	12.8	12.8	12.8	12.7	12.5	12.6	12.6	12.3
II	14.9	14.6	14.5	14.4	14.6	14.5	14.2	14.2	14.4	14.1
III	17.1	17.0	16.9	16.9	16.9	16.9	16.6	16.9	16.9	
IV	18.1	17.9	17.9	17.9	17.8	17.8	17.8	17.9	17.8	17.6
V	22.1	21.6	21.1	21.1	21.3	21.0	20.9	21.2	20.9	20.3
Va	23	23.9	23.4	23.4	23.6	23.6	23.1	23.3	23.2	23.2
VI[b]	28.1	27.9	28.1	28.1	27.9	27.5	27.5	27.6	27.7	27.2
R	0.72	0.81	0.66	0.69	0.75	0.37	0.54	0.64	0.42	0.24

[a] I through Va ±0.1 kK; 1 kK = 1000 cm^{-1}.
[b] ±0.2 kK.

anions give maxima at lower energy. The results, of course, may be interpreted in a number of ways. From the previous spectral studies, it is known that porphyrins with the highest negative charge in the macrocycle give the highest energy transitions. Further, the anion shifts are not specific but most likely relate to changes in all the porphyrin levels. Therefore, the high energy shift noted for some anions can be interpreted to arise from an increase in charge in the porphyrin ligand and, vice versa, a low energy shift can be correlated to a lower negative charge in the porphyrin. If this is so, then the axial anion controls, to a small extent, the charge in the porphyrin. A mechanism for this would involve controlling the charge on the metal. Hard anions prefer a high charge on the metal to give a strong ionic interaction, while soft anions allow a low charge on the metal. In the first instance, a high positive charge on the metal means a high negative charge on the porphyrin. In the second instance, the low charge on the metal means low charge on the porphyrin. Implicit in the argument is the assumption that little or no charge donation occurs from the axial anion to the metal, i.e. that the axial interaction is largely ionic and no significant σ or π mixing occurs between the metal *d*-orbitals and the axial anion. There are, of course, other factors which may be important in influencing the frequencies of the absorption maxima. For example, anion–porphyrin "charge transfer" interactions may lead to the observed band shifts. The $\pi \rightarrow \pi^*$ transitions of the porphyrin involve substantial charge reorganization [45]. Polarizable axial anions can stabilize the excited state and lower the energy of the transitions. This may be an important factor in accounting for the low-energy transitions of the complexes for the highly polarizable iodide ion.

The latter effect may also be operating in the moderate solvent shifts that are noted for Mn^{III} porphyrin spectra. Solvents can be divided into two classes, coordinating solvents and non-coordinating solvents. In the latter group the axial anions remain bound to the metal since the spectra are still anion-dependent while in the former, the anion is displaced and the axial coordination positions are filled by two solvent molecules. Spectra of [Mn(DMPrpor)(I)H_2O] [47] and [Mn(DMMesopor)(OH)H_2O] [29] were determined in a number of weakly coordinating solvents. The frequencies of the absorption maxima, which all shift in the same direction, vary with the solvent. The most sensitive absorption, bands V and VI, show a range of shifts of 0.3–0.4 kK for the OH^- and 0.7 kK, 1.6 kK for the iodide. A combined order is

$$CH_3\overset{O}{\overset{\|}{C}}CH_3 > CH_3CN > (C_2H_5)_2O > CH_3NO_2 > CH_3CO_3C_2H_5 > C_6H_{12} > CH_2Cl_2 \sim CHCl_3 > CCl_4 > C_6H_6 \qquad (10)$$

The order corresponds to the refractive index of the solvent; i.e. the lowest refractive index solvent (least polarizable) gives the highest energy absorption [52]. A solvent effect is expected for aromatic molecules like porphyrins [51]. It is interesting to note that the solvent dependence of the spectra is of comparable magnitude to that of the anions. Further, the complex with the polarizable anion, iodide, shows enhanced sensitivity to the solvent. The formation of charge-transfer complexes with donor and acceptor molecules also shifts the absorption bands of [Mn(DMMesopor)(OH)H_2O] in methylene chloride by as much as 0.6 kK [29].

Spectra were measured for [Mn(DMMesopor)(OH)H_2O] [29] and [Mn(DMPrpor)(X)H_2O] [47]

in good coordinating solvents. As expected, the spectra are independent of anion in these solvents. The donor solvent order for band V is

$$H_2O > C_2H_5OH \sim CH_3OH > C_6H_{11}OH \sim CH_3\overset{O}{\overset{\|}{S}}CH_3 \sim H\overset{O}{\overset{\|}{C}}N(CH_3)_2 \sim n\text{-}C_4H_9NH_2 > Py \quad (11)$$

It is readily seen that the oxygen donors give higher energy bands than the nitrogen donors. This is in general agreement with the findings of the anion order. The shifts within the oxygen donor class are small, ~0.2 kK, while the difference between the oxygen donors and pyridine is somewhat larger, ~0.7 kK. A general solvent effect may also be superimposed on this ligand-binding effect. The spectra of the solvent complexes show some additional features. A typical spectrum of a pyridine solution is shown in Fig. 4. Bands I and II can be resolved into a number of components. For example, a high-energy shoulder can be clearly seen on band I, and band II appears to be composed of three components. In general, the components are not clearly resolved in chloroform solution.

In addition to the studies cited above, a number of absorption spectra of Mn^{III} porphyrins have been recorded. For example, the visible spectra of $[Mn(Hpor)(OH)H_2O]$ [10] and $[Mn(DMHpor)(OH)H_2O]$ [14] in glacial acetic acid have been reported. The superimposition of the spectra indicate that the free acid porphyrin complex and dimethylester–porphyrin complex show the same spectrum in a common solvent. The lack of sensitivity of the absorption spectrum to β substituents removed from direct attachment

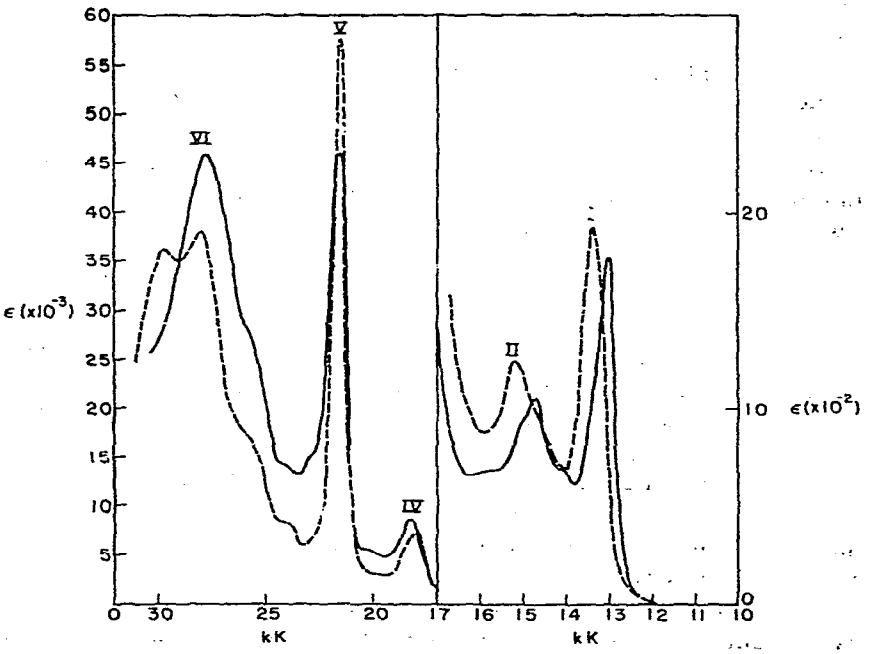

Fig. 4. Absorption spectrum of chloro(aquo)porphinemanganese(III) in pyridine(——) and chloroform (– – –).

to the ring is also exemplified in the spectrum for [Mn(OEP)(Cl)H_2O] [22] in methylene chloride. The absorption maxima appear close to those of the other fully alkylated porphyrins like Etio and DMMesopor [34]. The spectra of [Mn(TPP)(Cl)H_2O] [49] in methylene chloride and [Mn(Etio)($C_2H_3O_2$)$C_2H_4O_2$] [26] and [Mn(Mesopor)(OH)H_2O] [12] in pyridine agree with those reported [34]. On the other hand, the spectrum of [Mn(DMMesopor)(Cl)H_2O] in chloroform does not agree with that determined later [38]. Absorption spectra have also been measured at 300°C for [Mn(OEP)(Cl)H_2O], [Mn(OEP)($C_2H_5O_2$)H_2O] and [Mn(TPP(Cl)H_2O] in silicone oil. While all the maxima broaden and bands V and VI remain about constant, bands III and IV move to lower energy (~ 0.3 kK) in comparison with room-temperature spectra [22]. Attempts to measure vapor-phase spectra in vacuo lead to the formation of Mn^{II} porphyrins [22,50].

Magnetic circular dichroism spectra have proved to be extremely useful in unravelling metalloporphyrin electronic spectroscopy [53]. The MCD spectra of normal metalloporphyrins are dominated by strong *A* terms at the absorption maximum at both the *Q* (one strong and one weak for the vibrational components) and *B* bands [53]. This arises naturally because the transitions involve a double degenerate level, e_g^*. The MCD spectra of several Mn^{III} porphyrins have been determined [34,54]. The MCD and absorption spectra from 15 to 30 kK of [Mn(Etio)(Cl)H_2O] are reproduced in Fig. 5. In this case, the spectrum cannot be described simply with *A* terms but must also include *B* and *C* terms (for transitions among non-degenerate levels). Bands III, IV and V do, however, give rise to strong *A* terms. On the other hand, band VI clearly does not show an *A* term, giving an MCD maximum at the absorption maximum. Shoulders on either side of band VI also give rise to MCD maxima. Finally, band Va shows a non-*A* term. A recent study has explored the MCD spectra in the region of bands I and II [54]. It is found that band I gives rise to an *A* term and band II to a *B* term. There is also a *B* term on the high-energy shoulder of band I and in pyridine solution a splitting of band II gives rise to two *B* terms of opposite sign. All the results can be interpreted in the following way. Bands I, III, IV and V arise from transitions involving a doubly degenerate level. On the other hand, bands II and Va arise from transitions involving singly degenerate levels. Further, the complex MCD pattern at band VI implies that several transitions which are magnetically mixed give rise to the absorption. Further work on MCD spectra of Mn^{III} porphyrins will obviously be extremely useful.

Although Mn^{III} porphyrins do not show any observable fluorescence spectra [38], a phosphorescence spectrum of [Mn(DMMesopor)($C_2H_3O_2$)H_2O] in a rigid EPAF glass, of 0.5 part *N,N*-dimethylformamide, 3 parts ethanol, 6 parts ether and 5 parts isopentane, at 77°K, has been reported [23]. The spectrum shows a strong band at 15.2 kK and a weak band at 14.7 kK. The posphorescence quantum yield was found to be very small and the triplet-state lifetime to be very short (< 0.5 msec). As yet, this result has not been confirmed by excitation-spectra measurements. Recent work in both the experimental determination and the theory of luminescent spectra of metalloporphyrins has shown the spectra are quite sensitive to the metal ion and presumably to the metal porphyrin interaction [49]. A study of phosphorescence spectra of various Mn^{III} porphyrins may prove to be valuable in understanding the electronic structure of these materials.

Although a great amount of research has been carried out on the electronic absorption spectroscopy of Mn^{III} porphyrins, much detailed work remains to be done. Up to this point, the work has shown that the spectra of Mn^{III} porphyrins are sensitive to porphyrin,

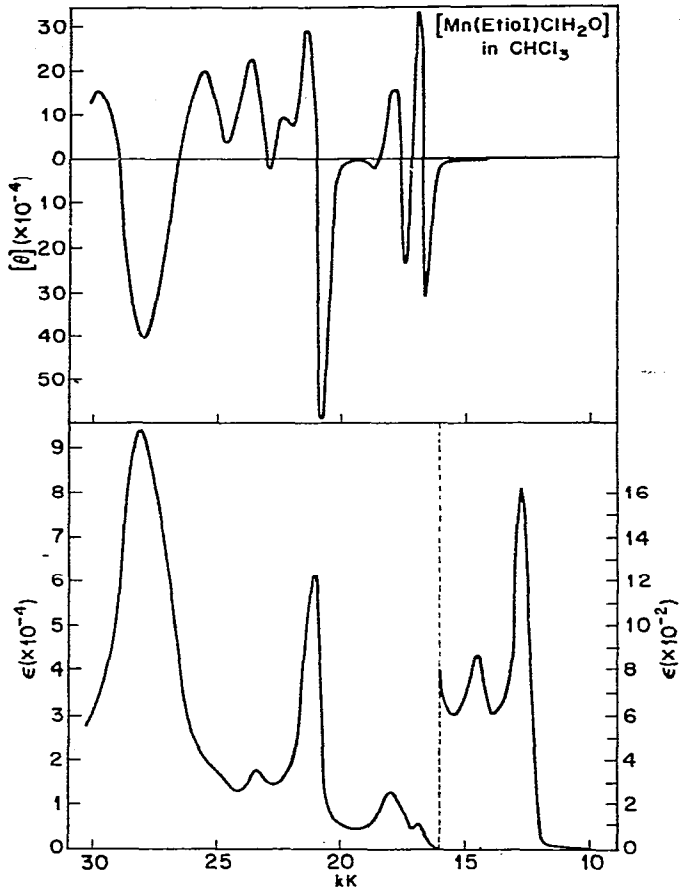

Fig. 5. MCD spectrum at 65 KG, and absorption spectrum of chloro(aquo)etioporphyrin I manganese(III) in chloroform.

anion, additional donor molecules and solvent. Although a rationalization of the effects can be made, the complexity of the Mn^{III} porphyrin system thwarts any more than naïve discussion.

(iv) Electronic structure

The anomalous absorption spectrum of Mn^{III} porphyrins, i.e. the disruption of the normal metalloporphyrin $\pi \rightarrow \pi^*$ spectrum, can be related to a strong metal–porphyrin π interaction. For metal ions, with effective D_{4h} symmetry, the $e_g(d_{xz}, d_{yz})$ orbital is of proper symmetry to interact with the $e_g^*(\pi)$ orbital on the porphyrin. The most favorable geometry for metal–ligand π overlap occurs when the metal is in the plane of the porphyrin [55]. This also leads to the strongest sigma interaction between the metal and the four pyrrole nitrogen donors of the porphyrin. The strong sigma bonding is undoubtedly the most important interaction in metalloporphyrins. However, the existence of moderate back π bonding from the metal to the porphyrin helps relieve the charge build-up on the

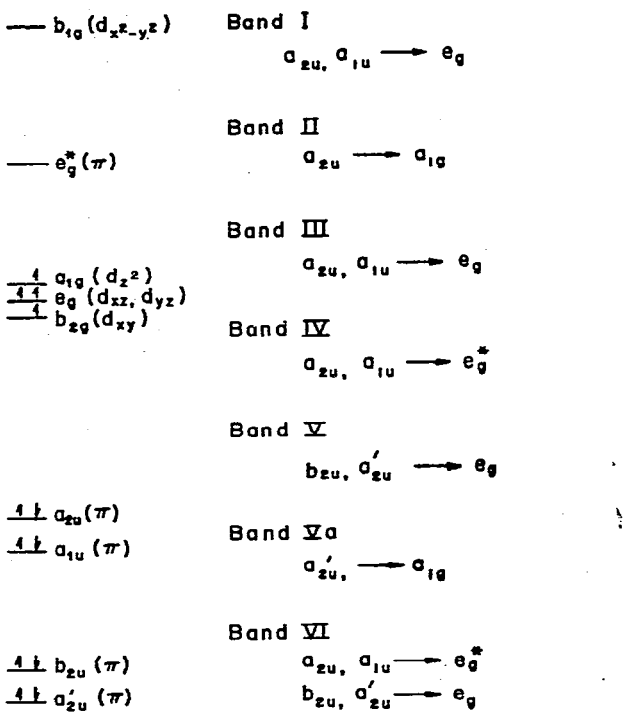

Fig. 6. Qualitative molecular orbital level diagram and visible absorption band assignments for Mn^{III} porphyrins.

metal atom that results from sigma donation. Thus the metal–porphyrin bond can be considerably strengthened. This is another example of the well-known synergic bonding in metal complexes [56]. Theoretical calculations predict that the metal *d* orbitals will match in energy the porphyrin π levels somewhere in the first transition series since the *d* levels are very high in energy at Ca^{II} and very low in energy at Zn^{II} (ref. 44). It appears that this match may occur around manganese and iron. Thus Mn^{III} porphyrins would show strong metal $e_g(\pi)$ porphyrin $e_g^*(\pi)$ mixing. The model developed below is based on this contention.

A qualitative molecular orbital energy level diagram for Mn^{III} porphyrins is given in Fig. 6 and is analogous to the energy-level scheme obtained for Fe^{III} porphyrins [56]. Since all the Mn^{III} porphyrins have a high-spin d^4 configuration, the four lowest *d*-orbitals are singly occupied and the strongly antibonding b_{1g} orbital remains empty. The energy of the a_{1g} metal level will depend on the axial anion while the b_{2g} level is non-bonding. Since no anions give rise to low-spin complexes, axial interactions must not be strong enough to give spin pairing (by raising the a_{1g} in energy). This is probably a consequence of the strong in-plane porphyrin interaction. The $e_g(d\pi)$ metal level is depressed in energy because it is π bonding to the porphyrin. In an analogous way, the porphyrin $e_g^*(\pi)$ level is raised in energy because it is antibonding with respect to the π interaction.

As a consequence of the metal–porphyrin π mixing, not only should the $\pi \rightarrow \pi^*$ spec-

trum be altered, but a number of charge-transfer bands should gain intensity and be observed in the spectrum. The allowed low-energy charge-transfer bands are the porphyrin-to-metal [56] bands.

$a_{2u}(\pi) \rightarrow e_g(\pi)$

$a_{1u}(\pi) \rightarrow e_g(d\pi)$

$b_{2u}(\pi) \rightarrow e_g(d\pi)$

$a'_{2u}(\pi) \rightarrow e_g(d\pi)$

$a_{2u}(\pi) \rightarrow a_{1g}(d_{z^2})$

$a'_{2u}(\pi) \rightarrow a_{1g}(d_{z^2})$

In addition, the visible spectrum should show the porphyrin $a_{1u}, a_{2u} \rightarrow e_g^*$ bands. A tentative assignment of the prominent visible absorption bands of Mn^{III} porphyrins is given in Fig. 6. The lowest energy band, I, can be assigned to the low energy part of the a_{1u}, $a_{2u} \rightarrow e_g$ charge-transfer transition. The high energy part of the pair of transitions that are mixed by configuration interaction would be band III. Further, band V can be assigned to the low-energy component of the $a'_{2u}, b_{2u} \rightarrow e_g$ charge transfer. The less intense bands, II and Va, can be assigned to $a_{2u} \rightarrow d_{z^2}$ and $a'_{2u} \rightarrow d_{z^2}$ charge-transfer transitions. Band IV would then be assigned to the low-energy component of the $a_{1u}, a_{2u} \rightarrow e_g^*$ porphyrin transition. This pair of transitions should be heavily mixed by configuration interaction as with other metalloporphyrins. Similarly, the $b_{2u}, a'_{2u} \rightarrow e_g$ transition may be mixed. Band VI still remains to be assigned. A reasonable assumption would be that it arises from the high-energy component of $a_{1u}, a_{2u} \rightarrow e_g^*$ and from the high-energy part of $a'_{2u}, b_{2u} \rightarrow e_g$. The two transitions would be similar in energy and will couple to give the observed broad band [58]. The relative intensity of all the bands will depend in a complicated way on the transition dipoles of the pure configuration and on the extent of mixing.

While the experimental data do not prove the above assignment scheme, much of the information is consistent with it. Bands I and II are of low intensity and energy as required by the assignment to charge-transfer bands. Further, they show the expected A term for band I and the B term for band II since the first band involves transition to a doubly degenerate $d\pi$ level and band II only involves singly degenerate levels. It is tempting to assign bands III and IV to the vibrational components of a Q band. There are several reasons in favor of only assigning band III to an $a_{1u}, a_{2u} \rightarrow e_g$ band. The separation of band III and band IV is smaller than the vibrational components of the Q band [45], and both bands III and IV show sharp A terms of near equal magnitude. Conversely, the MCD spectra of divalent metalloporphyrins show only one strong A term for the Q bands and a much weaker one on the high-energy side. It therefore seems reasonable to assign band IV to a Q band, $a_{1u}, a_{2u} \rightarrow e_g^*$. The sharp A term for band V also supports the notion that this is a $b_{2u}, a'_{2u} \rightarrow e_g$ transition. As expected, band Va shows a non-A term. The MCD spectrum at band VI quite clearly does not show the normal A term which could be associated with a B porphyrin transition. The observed MCD pattern may arise from mixing of the B band, $a_{1u}, a_{2u} \rightarrow e_g^*$, with the charge transfer band $b_{2u}, a'_{2u} \rightarrow e_g$ of similar energy which is induced by the external magnetic field. The intensity of the charge transfer bands

of the Mn^{III} porphyrin absorption spectra is surprisingly high. This can be attributed to the substantial porphyrin (π) character of the $e_g(d\pi)$ level. Conversely, the intensity of the $\pi \rightarrow \pi^*$ bands is lower than usual since the $e_g^*(\pi)$ level is no longer a pure porphyrin orbital. In agreement with the destabilization of the e_g^* level via metal–porphyrin back π bonding, the $a_{1u}, a_{2u} \rightarrow e_g^*$ transitions, bands IV and VI are at higher energy than for normal metalloporphyrins. The intensity of charge-transfer bands II and Va in the spectrum may arise from some porphyrin π mixing into the metal d_{z^2} orbital [57].

An alternative assignment of bands I and II has recently been made [59]. In this study, the bands are assigned to manganese $d \rightarrow d$ transitions. In a D_{4h} symmetry field the degenerate d-levels of Mn^{III} are split and three spin-allowed transitions are expected: $d_{z^2} \rightarrow d_{x^2-y^2}, d_{xz}, d_{yz} \rightarrow d_{x^2-y^2}$ and $d_{xy} \rightarrow d_{x^2-y^2}$. Bands I and II can then be assigned to the first d–d transitions. There are a number of objections to this ligand field analysis. For one, the intensity of bands I and II are between one and two orders of magnitude higher than observed for normal d–d transitions of Mn^{III} complexes [60]. In fact, they are more in the range expected for charge-transfer bands [61]. Secondly, the analysis assumes that the d levels in the complex are essentially pure metal levels. The anomalous visible spectrum of Mn^{III} porphyrin shows that there is substantial mixing of the porphyrin levels into the metal levels. The MCD spectra settle the point about band I since the observed A term rules out a $d_{z^2} \rightarrow d_{x^2-y^2}$ transition. Nevertheless, the additional features observed near bands I and II (which are somewhat better resolved in pyridine solution) might be due to the low energy $d \rightarrow d$ transition. Polarized absorption spectra and optical activity measurements of Mn^{III} porphyrins, in a protein, would aid in picking out any $d \rightarrow d$ transition buried under the charge-transfer bands [62,63].

The anion dependence of the intensity of the absorption maxima may be related to metal–porphyrin π mixing. Hard acid anions stabilize a high positive charge on the metal atom with the resulting high charge in the porphyrin. Since sigma donation is probably going to be strong in any case, the increase in charge in the porphyrin can be related to the back π bonding of the metal to the porphyrin. In this case, π bonding should be strong and the charge-transfer bands are intense. Conversely, with soft anions, the metal porphyrin charges are low. Back bonding to the prophyrin is poor and the intensity of the bands is low. The intensity changes when going from the hydroxide to the iodide complex are are consistent with this proposal. The anion dependence of the energy and intensity of the absorption maxima may also be due to differences in coordination geometry. With small axial anions like fluoride, the metal may be in the plane of the porphyrin. Conversely, with large anions like iodide the metal may be considerably out of plane and other anion complexes would fall between the two extremes. In the in-plane case, back π bonding would be strong and the charge transfer bonds intense. Another consequence of this would be a high negative charge in the porphyrin and blue shifted absorption bands. In the out-of-plane case, back π bonding would be weaker and the charge transfer bands relatively less intense. Further back donation would be less with charge build-up in the porphyrin rather small. Hence, a red-shifted spectrum would result. Detailed structural work must be done before this argument can be more fully discussed.

(v) Molecular structure

The structures of a large number of metalloporphyrins have now been elaborated [28].

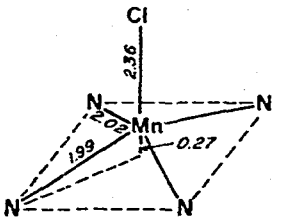

Fig. 7. Structural representation of (chloro)-α,β,γ,δ-tetraphenylporphinemanganese(III).

Unfortunately, only one structure of an Mn^{III} porphyrin has been completely solved. Some bond distances for [Mn(TPP)Cl] [64] are given in Fig. 7. The crystallographic data are

Space group monoclinic $P2_{1/c}$

4 molecules per unit cell

$a = 14.56$ Å
$b = 21.77$
$c = 17.01$
$\beta = 135.6°$

The porphyrin molecules in the crystal are stacked approximately perpendicular to the $\vec{c}^*$ direction with an acetone molecule of crystallization trapped between adjacent porphyrin molecules.

The coordination sphere of the [Mn(TPP)Cl] is composed of a five-coordinate Mn^{III} surrounded by a square pyramidal array of four pyrrole nitrogens in the base and an axial chloride ion. No coordinated water molecule is seen. The axial chloride ion is coordinated to the metal atom at a bond distance of 2.36 Å, approximately perpendicular to the mean plane of the four basal nitrogen atoms (angle 86°). The four nitrogens are alternately at a bond distance of 2.02 Å and 1.99 Å (2.01 average) from the manganese. Finally, the manganese is above the mean plane of the four basal nitrogen atoms by 0.27 Å toward the axial chloride ion. The distances can be contrasted to those of the analogous [Fe(TPP)Cl] [65]: Fe–Cl 2.19 Å; Fe–N 2.05 Å; out-of-plane 0.38 Å and the porphyrin skeleton essentially planar. Even though the two metal ions are of comparable size (within 0.01 Å for high-spin six-coordinate structures) [66] the distances are significantly different; e.g., the axial bond is considerably longer, 0.17 Å, and the in-plane bond a little shorter, 0.04 Å, for the Mn^{III} derivative. This finding is consistent with the model proposed here. Porphyrin π bonding gives a strong Mn–N interaction (a short bond) while the resulting weak axial interaction then gives a rather long axial bond. It must be pointed out, however, that the Mn–Cl distance is just a little shorter than the sum of the ionic radii, 2.40 Å. The question remains as to why the manganese is out of the plane of the porphyrin. Molecular orbital considerations place no restriction on the metal being in the porphyrin plane for high-spin d^4 cases since the $d_{x^2-y^2}$ orbital is not populated [56]. The out-of-plane displacement may be related to the overlarge size of the high-spin Mn^{III} and the resistance of the porphyrin skeleton to expand to accept it in a planar configuration. Another factor may be the large size of the axial chloride ion. In order to maintain even a weak bond with

the metal and avoid strong repulsive forces with the porphyrin nitrogen atoms the anion "pulls" the metal out of the plane towards itself. With a smaller anion the metal would then be expected to be in the plane. It is interesting to note that the out-of-plane displacement is 0.11 Å less in the Mn^{III} than in the Fe^{III} case. Again, this is consistent with a strong porphyrin interaction in the former complex.

While the bond lengths are all normal for a metalloporphyrin [29] and the pyrrole rings are planar, the porphyrin skeleton in [Mn(TPP)Cl] is decidedly non-planar. The four porphyrin pyrrole nitrogens are alternately above and below the NLS (nuclear least squares) plane of the porphyrin skeleton by 0.04 Å. Further, the β carbon atoms in the pyrrole rings are alternately up and down, 0.3–0.5 Å from the NLS plane. The other atoms, α and methine carbons of the porphyrin, are also significantly out of this plane, 0.05–0.25 Å. In other words, the porphyrin skeleton is highly ruffled in the solid state, much like the cation H_4TPP^{2+} (ref. 67). Whether this distortion arises from packing forces in the solid or from specific bonding interaction is uncertain. The observed ruffling of the porphyrin skeleton may be related to the requirement of a short Mn–N bond while maintaining the metal out of plane. The nitrogen to center of the porphyrin ring distance is 1.99 Å in the Mn^{III} structure. This is 0.02 Å shorter than in [Fe(TPP)Cl]. The solid-state structure shows two different kinds of β substituents, one up toward the metal and one down on the other side of the porphyrin from the metal. If the structures are maintained in solution, these should be spectroscopically distinguishable, e.g. by NMR.

(vi) Reduction

The reaction of an appropriate reducing agent with Mn^{III} porphyrin rapidly yields the corresponding Mn^{II} complexes [18]. A similar process can be carried out by electrochemical electrolysis [22]. The potential for this one-electron reversible reduction has been determined by potentiometric titration and polarographic measurements. Some of the data are summarized in Table 3. The concentration range used was 10^{-4} to 10^{-5} *M* where it is assumed that aggregation effects will not be important. The potential for [Mn(Hpor)(OH)H_2O] reduction determined polarographically at the dropping mercury electrode [68] agrees reasonably well with that determined potentiometrically [10]. The redox potential varies with pH in aqueous solution and detailed examination of the data shows the variation to be consistent with a redox-linked proton function (6) [10]. In contrast, no pH dependence is noted when additional ligands (1–2*M*) are present [12]. Under these conditions, the species being reduced is the bis ligand complex [12,68]. The redox potential order, $-E$, for aqueous solution is

$$\text{Imidazole} > OH^- > \text{Py} > \gamma\text{-picoline} > \beta\text{-picoline} > \alpha\text{-picoline} > \text{nicotine} \quad (12)$$

The polarographic reduction [19] of [Mn(Etio)(X)H_2O] and [Mn(Prpor)(X)H_2O] in acetonitrile yields the following, $-E$, orders

$$\text{Etio} > \text{DMMesopor} > \text{DMDepor} > \text{DMHpor} > \text{DMPrpor} > \text{TPP} \quad (13)$$

$$F^- > C_2H_3O_2^- \sim N_3^- > OCN^- > OH^- \sim Cl^- > Br^- > SCN^- > I^- \quad (14)$$

TABLE 3

Potentials [a] for $Mn^{III} \rightarrow Mn^{II}$ reductions of manganese porphyrins

Complex	Solvent [b]	T (°C)	Added ligand	E (V)	Method	Ref.
[Mn(Hpor)(OH)H_2O]	H_2O (μ = 0.3)	22.5		−0.357	PT [c]	10
[Mn(DMHpor)(Cl)H_2O]	20% Ethanol–H_2O (μ = 0.3)			−0.268	PT	10
[Mn(Mesopor)(OH)H_2O]	H_2O (μ = 0.1)	30	α-Picoline	−0.296	PT	12
			Pyridine	−0.37	PT	12
			Nicotine	−0.28	PT	12
[Mn(Hpor)(OH)H_2O]	10% Ethanol–H_2O (μ = 1.2)	25		−0.343	PL	68
	H_2O		Pyridine	−0.280	PL	68
			α-Picoline	−0.225	PL	68
			β-Picoline	−0.254	PL	68
			γ-Picoline	−0.259	PL	68
	20% Ethanol–H_2O		Imidazole	−0.353	PL	68
	H_2O		Nicotine	−0.231	PL	68
[Mn(Etio)(Cl)H_2O]	CH_3CN (μ = 0.1)	25		−0.21	PL	19
[Mn(DMMesopor)(Cl)H_2O]				−0.19	PL	19
[Mn(DMDepor)(Cl)H_2O]				−0.14	PL	19
[Mn(DMHpor)(Cl)H_2O]				−0.13	PL	19
[Mn(DMPrpor)(Cl)H_2O]				−0.11	PL	19
[Mn(TPP)(Cl)H_2O]				+0.01	PL	19
[Mn(Etio)(F)H_2O]				−0.25	PL	19
[Mn(Etio)(Br)H_2O]				−0.17	PL	19
[Mn(Etio)(I)H_2O]				−0.05	PL	19
[Mn(Etio)($C_2H_3O_2$)H_2O]				−0.24	PL	19
[Mn(Etio)(OH)H_2O]				−0.21	PL	19
[Mn(Etio)(N_3)H_2O]				−0.24	PL	19
[Mn(Etio)(SCN)H_2O]				−0.16	PL	19
[Mn(Etio)(OCN)H_2O]				−0.22	PL	19
[Mn($Mepheo_a$)(Cl)H_2O]	20% EtOH–H_2O (μ = 0.3)	22.5		−0.181	PT	89
[Mn($Mepheo_a$)(Cl)H_2O]	CH_3CN (μ = 0.1)	25		+0.01	PL	89
[Mn_2(PC)$_2$(Py)$_2O$]	Py (μ = 0.05)			−0.64	PL	100

[a] Versus standard hydrogen electrode.
[b] Aqueous solutions, pH 9.0.
[c] PT potentiometrically, PL polarographically.

The same porphyrin order is obtained for dimethylformamide solutions [19]. In aqueous solution the order is Mesopor > Hpor [10,12].

The redox-potential order for the various porphyrins corresponds to the pK_a order, i.e. the higher the basicity of the porphyrin, the more negative the redox potential. This shows that the Mn^{III} is stabilized by strong in-plane sigma donation from the porphyrin. It is significant that the redox-potential order for the various anion complexes approximately follows the hard base character of the anion. In fact, the frequency order from the visible absorption spectra corresponds to the redox-potential order. The smooth correlation between the two quantities is nicely shown in Fig. 8. The most electronegative species, F^-, gives the most negative redox potential while the least electronegative species, I^-, gives the most positive potential. Hard bases stabilize Mn^{III} porphyrins to reduction more than do soft bases. The observation that the sigma donating ability of added ligand molecules is not related to the stability of Mn^{III} porphyrins [68] is also consistent with the relative unimportance of sigma bonding ability of the axial ligands. From the limited data available the anion order (14) is also the order for stability constants of Mn^{III} complexes [69]. In a general way, then, the axial ligand which forms the strongest bond to the metal stabilizes the +3 oxidation state to the greatest extent. Both the anion and porphyrin trend noted here reflect the common observation that strongly binding ligands stabilize the high oxidation states of transition metal ions [70]. Also implicit in this discussion is the supposition that the axial interaction is largely ionic in character. It is interesting to note that the porphyrin ligand greatly stabilizes the Mn^{III} to reduction since the potential for the Mn^{III}/Mn^{II} half reaction in acidic solution is +1.5 V [9].

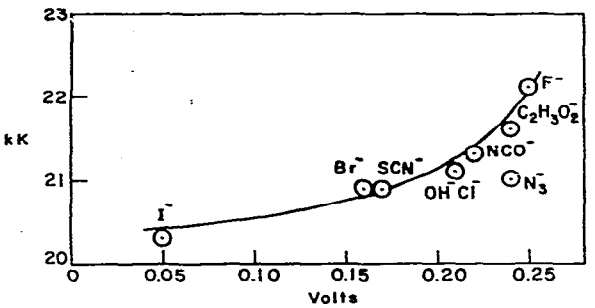

Fig. 8. Plot of the half-wave potential $E_{1/2}$ for acetonitrile solutions versus absorption maxima (band V) for chloroform solutions of anion(aquo)etioporphyrin I manganese(III).

The rate of reduction at 25°C of [Mn(TPPy)(OH)H_2O], in aqueous solution at a pH 2.0, $\mu = 1.0$, has been determined for several reducing agents [20]. The second-order rate constants are $8.40 \times 10^2\ M^{-1}.sec^{-1}$ for Cr^{II}, $1.45 \times 10^2\ M^{-1}.sec^{-1}$ for V^{II} and $1.29 \times 10^3\ M^{-1}.sec^{-1}$ for $[Cr(bipy)_3]^{2+}$. When added anions like Cl^- or NCS^- are present, the rates of reduction increase from one to three orders of magnitude. The reaction rates then show a first-order dependence on the anion concentration. This may arise from an anion Mn^{III} porphyrin or reducing agent complexation occurring in a rapid pre-equilibrium step. The third-order rate constants are Cl^-, Cr^{II}, $3.05 \times 10^3\ M^{-2}.sec^{-2}$, Cl^-, $V^{II} < 10^3\ M^{-2}.sec^{-1}$ and for SCN^-, Cr^{II}, $2.7 \times 10^5\ M^{-2}.sec^{-1}$, SCN^-, V^{II}, $4.2 \times 10^5\ M^{-2}.sec^{-1}$. Unfortunately, insufficient

information exists to deduce a detailed mechanism for the redox reaction, i.e. whether they are inner sphere or outer sphere in character [71]. The rates of reduction noted for Mn^{III} porphyrins are, however, comparable to those of other Mn^{III} complexes [69].

The Mn^{III} porphyrins are also reduced in the vapor phase at elevated temperatures. For example, when $[Mn(OEP)(Cl)H_2O]$ is vaporized in vacuo at ~400°C, the only species spectrally noted in the gas phase is the Mn^{II} derivative [22]. For $[Mn(TPP)(Cl)H_2O]$ the spontaneous reduction is somewhat slower, taking ~ 10 min for completion in the gas phase [49]. The same reduction process results during the vacuum sublimation of $[Mn(Etio)(C_2H_3O_2)H_2O]$ [25] and during the determination of the mass spectrum of $[Mn(TPP)(Cl)H_2O]$ and $[Mn(OEP)(Cl)H_2O]$ [22]. The spontaneous reduction is apparently the rule for trivalent transition metal porphyrin complexes [26]. The mechanism of this process is at present unknown. The photochemical reduction of $[Mn(Etio)(C_2H_3O_2)C_2H_4O_2]$ in pyridine solution has also been reported [72]. The solutions, in the absence of oxygen, were exposed to white light for varying periods of time with a flood lamp which was filtered through water to remove infrared radiation. The product obtained was $[Mn(Etio)Py_2]$ and no porphyrin alteration was noted. Although somewhat variable, the first-order rate constant at 25°C was $\sim 6 \times 10^{-4}$ sec^{-1} (ref. 73). The presence of water (up to 20%) in the pyridine slows the reduction down somewhat. However, reoxidation occurs when illumination ceases, at a rate about one-tenth as fast as the reduction. Ethanol solutions of $[Mn(Etio)(C_2H_3O_2)C_2H_4O_2]$ saturated with sodium cyanide and in the absence of air are also reduced in sunlight [26]. Information about these very interesting photoreductions is as yet sketchy. The influence of solvent, porphyrin complex and wave length of the light are still to be determined. It is interesting to note that other Mn^{III} complexes are generally found to undergo facile photochemical reduction when illuminated by visible light in solution or the solid state [74].

C. MANGANESE(II) PORPHYRINS

Although no procedure for the preparation and isolation of pure solid Mn^{II} porphyrins has been published, these materials can be easily generated in situ and their properties studied. Formation of the materials involves chemical reduction with $Na_2S_2O_4$ in pyridine–water or water at pH ~ 11 (ref. 18) or electrochemical reduction in methylene chloride solution at a platinum electrode [22], of the corresponding Mn^{III} porphyrins. If these solutions are protected from air, the spectral properties of the materials can be easily determined. In the presence of air, however, the complexes are rapidly oxidized to the Mn^{III} complex. Even in the absence of air, aqueous solutions of Mn^{II} porphyrins slowly demetallate; i.e. the complex decomposes to give the aquated Mn^{II} ion and free porphyrin ligand. This reaction is acid-catalyzed and found to be first-order in H^+. The first-order rate constant at 25°C for decomposition of $[Mn(Hpor)(OH)H_2O]$, in 45% ethanol–water $\mu = 1.0$, is $k_1 = 8 \times 10^{-6}$ sec^{-1} at pH 7, and 1×10^{-1} sec^{-1} at pH 3.4 (ref. 22). While half-time for dissociation at pH 7 is ~ 30 h, at pH 6 it is only ~ 20 min. The mechanism of the demetallation proposed involves the rapid formation of a protonated intermediate, followed by a slow rate-determining expulsion of the Mn^{II}. The intermediate is thought to have a protonated pyrrole nitrogen with the metal considerably out of the plane of the porphyrin. In aprotic solvents, demetallation is not observed. The coordination number of

Mn^{II} porphyrins is at present uncertain. By analogy with divalent metalloporphyrins it is probably six in coordinating solvents like pyridine and water; i.e. there are two axial ligands bound to the metal [22,75]. One axial ligand is probably more tightly held than the second [22,75] Potentiometric and spectrophotometric measurements are consistent with the binding of two pyridine molecules with an overall stability constant

$$[Mn(Mesopor)(H_2O)_2] + 2\,Py \rightleftarrows [Mn(Mesopor)Py_2] + 2\,H_2O \qquad (15)$$

of $K = 38$ at 30°C, pH 7 (ref. 22). This is more than two orders of magnitude larger than the value for the Mn^{III} complex [12]. Of course K is the product of K_1 and K_2, the stability constants for the addition of the first pyridine molecule and for the addition of the second ligand. Unfortunately, the individual stability constants have not been determined. The ratio of the stability constant for the addition of two pyridine molecules to $[Mn(Hpor)(H_2O)_2]$ and to $[Mn(Hpor)(OH)H_2O]$ in 1 *M* pyridine at pH 9.0 at 25°C is 6.8 while the value for nicotine is 55. In general then, axial ligands bind more strongly to Mn^{II} porphyrins than to the Mn^{III} derivatives. The pK_a for the aqueous hydrolysis

$$[Mn(Hpor)(H_2O)_2] \rightleftarrows [Mn(Hpor)(H_2O)OH]^- + H^+ \qquad (16)$$

is found to be 12.8 (ref. 10). This value is somewhat larger than for the comparable Mn^{III} porphyrin. The ease of deprotonation of the coordinated water can be related to the increased positive charge of the higher oxidation state complex. When the M^{II} porphyrin is generated electrochemically in methylene chloride, the water originally associated with the Mn^{III} derivative may be present as a fifth ligand [22]. The same product, $[Mn(Por)H_2O]$, is probably formed during the vacuum sublimation of the Mn^{III} porphyrins. Exposure of a film of $[Mn(Etio)H_2O]$ to pyridine vapor gives rise to a shift in the absorption maxima, indicating a replacement of the axially bound water by one or more pyridine molecules [25].

Studies of the polarographic reduction of Mn^{II} porphyrins in acetonitrile and dimethylformamide have been made [19]. It is quite clear that the two polarographic waves seen at ~ -1.3 V and ~ -1.7 V are one-electron reversible reductions in which the electron enters the antibonding π orbital on the porphyrin. The half-wave potentials are dependent on the porphyrin in the same way as for the Mn^{III} reduction; i.e. they correspond to order (13). Electron-donating groups increase the electron density in the ring and reduction becomes more difficult. Ligand reduction potentials for a number of divalent metalloporphyrins have been measured and the Mn^{II} potentials fall into the region between those of Mg^{II} and Zn^{II} (ref. 76). The magnetic susceptibility of $[Mn(Hpor)H_2O)_2]$ has been measured for aqueous solutions, 0.1 *M* KOH, in the presence and absence of pyridine. In both cases, the magnetic moment was found to be 5.8–5.9 B.M. [10]. Previous reports of low magnetic moments are undoubtedly in error. The magnetic moments are consistent with a high-spin d^5 Mn^{II} complex with the configuration $b_{2g}{}^1 e_g{}^2 a_{1g}{}^1 b_{2g}{}^1$, i.e. one unpaired electron in each of the five *d* orbitals. The ESR spectrum of $[Mn(Propor)(H_2O)_2]$ embedded in Sephadex G-25 was examined at 77°K (ref. 77). The *x*-band spectrum shows two prominent signals at $g_\perp = 5.9$ and $g_\parallel = 2.0$ with the expected six $Mn(I=\frac{5}{2})$ nuclear hyperfine lines. The spectrum was analyzed as an $S=\frac{5}{2}$ system in an axial ligand field and the zero field splitting parameter, D, found to be 0.5 cm^{-1}. The spectrum also reveals a small rhombic

distortion in the molecules, but the quality did not allow a more detailed analysis.

The visible absorption spectra of a number of Mn^{II} porphyrins have been measured. A typical spectrum is shown in Fig. 2. The electronic spectra of Mn^{II} porphyrins are very similar to those of other divalent metalloporphyrins and show the usual α, β and Soret bands, e.g. at ca. 17.2, 18.2 and 23.5 kK, which can be assigned to the $a_{1u}, a_{2u} \rightarrow e_g^*(\pi \rightarrow \pi^*)$ transitions. The visible spectra of Mn^{II} porphyrins vary with solvent, porphyrin and phase and substituting one porphyrin for another produces shifts in all band frequencies [18]. The order of the band positions agrees with that observed for other divalent metalloporphyrins [48] and also for Mn^{III} porphyrins [34] (8). The bands also shift upon changes in axial coordination; e.g. the often observed frequency order $H_2O > OH^- > Py$ is noted [10,12]. There is also the expected substantial blue shift in going from solution to the gas phase for [Mn(OEP)H_2O] (ref. 22) and in going from the solution to a solid film for [Mn(Etio)H_2O] [25]. An additional feature of the spectra is the presence of very weak bands in the red end of the visible region, at 14.1 and ~15 kK. Presumably the bands arise from the allowed porphyrin-to-metal charge-transfer bands since Mn^{II} has no spin-allowed d–d transitions available. The bands are blue shifted and their intensity decreases by a factor of ten in going from Mn^{III} to Mn^{II}. The blue shift is a consequence of the destabilization of the metal d orbitals with the decrease in oxidation state and the intensity decrease is consistent with a decreased porphyrin π character in the $d\pi$ metal orbital. It is interesting to note an enhanced intensity and sharpening of the visible absorptions when going from Mn^{III} to Mn^{II}. This is consistent with the notion that there is considerable charge-transfer character in the bands of Mn^{III} but very little in the bands of Mn^{II}. The normal visible spectrum of Mn^{II} porphyrin strongly implies then that, like other divalent metalloporphyrins, there is little metal–porphyrin π mixing. Although no fluorescence spectra of Mn^{II} porphyrins have been observed, the phosphorescence spectrum of [Mn(DMMesopor)H_2O] in EPAF glass has been measured at 77°C. The spectrum shows bands at 13.3, 12.8 and 12.0 kK, but the result has not yet been confirmed by excitation spectral measurements.

In the high-spin Mn^{II} porphyrin, the strongly antibonding $d_{x^2-y^2}$ orbital is singly occupied. This orbital will be of low energy only if the metal is out of the plane of the porphyrin since sigma donation of the porphyrin to the metal falls off if the metal is removed from the plane [57]. Indirect evidence for this is the result of molecular orbital calculation which shows that planar configuration would give rise to an intermediate spin state [44]. More to the point, it is known that the isoelectronic high-spin Fe^{III} porphyrins adapt a non-planar configuration. The ease of demetallation of Mn^{II} porphyrin derivatives is also consistent with a structure in which the manganese metal atom is considerably out of the plane of the porphyrin. In this configuration, the porphyrin retains a high negative charge because of the poor sigma donation of the porphyrin to the metal and, as a consequence, the metal retains a high positive charge. The high potential of the Mn^{II} porphyrin ligand reduction is consistent with this description. Further, strong binding of an axial ligand is in line with the relatively high positive charge on the metal. The strong axial interactions and out-of-plane configuration are also consistent with the low zero field splitting for Mn^{II} porphyrins. The absorption maxima for Mn^{II} porphyrins appear near those of Mg^{II} porphyrins [78], the two divalent ions having similar sizes and electronegativities. Since Mn^{II} porphyrins are high-spin d^5 complexes, and crystal field effects are absent, it is reasonable to assume a similar molecular structure for the Mg^{II} complexes. The crystal and molecular

structure of the [Mg(TPP)H_2O] has been determined [79] and it is found that the metal atom is out of the plane of the porphyrin towards the single axial ligand [79]. A similar five-coordinate, out-of-plane structure may exist in the solid state and in solution in the absence of added donors for the Mn^{II} porphyrins. The lack of strong Mn^{II} porphyrin π mixing, which is suggested by the spectral data, may be at least partially ascribed to an out-of-plane structure.

D. MANGANESE(IV) PORPHYRINS

Addition of one equivalent of sodium hypochlorite to [Mn(Hpor)(OH)H_2O] at pH 13 rapidly yields a one-electron oxidation product that has been tentatively identified as an Mn^{IV} porphyrin [10]. The oxidation does not proceed at pH less than 9.0 with sodium hypochlorite or hydrogen peroxide. Potentiometric measurements yield an estimate of the oxidation potential for Mn^{III}–Mn^{IV} of +0.325 V at pH 13 and 22.5°C. The potential is pH-dependent and the reaction proceeds more readily in very alkaline solution. At pH 9.9, the oxidation potential is +0.635. From the pH dependence, the pK_a of the dissociation

$$[Mn(Hpor)(H_2O)_2]^{2+} \rightleftarrows [Mn(Hpor)(OH)_2] + 2H^+ \qquad (17)$$

is given as < 10. The great acidity of the coordinated water protons can be related to the high positive charge of the Mn^{IV} porphyrin. Several properties of the Mn^{IV} porphyrin have been determined. Susceptibility measurements on an aqueous solution of [Mn(Hpor)$(OH)_2$] yield magnetic moments of 2.0 B.M. This is slightly higher than expected for a low-spin d^3 case. A low-spin form for a d^3 metalloporphyrin is surprising since this would lead to the configuration $b_{2g}{}^2 e_g{}^1$. In most cases the splitting between those levels is too small to give spin pairing and the high-spin configuration $b_{2g}{}^1 e_g{}^2$ would be expected. Unfortunately, no ESR measurements have been made on the Mn^{IV} porphyrin.

Visible spectra of the Mn^{IV} porphyrins have been recorded. A typical spectrum is shown in Fig. 2. The materials show an intense peak at 25.1 kK as well as two weaker absorption bands at ~ 19 and 20.1 kK. Although somewhat broadened, these bands could arise from the normal metalloporphyrin *B* and *Q* bands. There are, however, several other absorptions in the spectrum; a weak one at 16.6 kK and a very weak, broad, low-energy band at 11.6 kK. A self-consistent picture would assign the low-energy bands to porphyrin-to-metal charge-transfer transitions. The increased stabilization of the metal *d* orbitals in the high-oxidation state naturally shifts these bands to lower energy than for the Mn^{III} porphyrins. The relatively normal $\pi \rightarrow \pi^*$ spectrum and low-intensity charge transfer band of the Mn^{IV} porphyrin would then indicate that metal–porphyrin π mixing is not strong. This is reasonable since the high-oxidation state would not be expected to be a good π donor to the porphyrin.

The Mn^{IV} porphyrins are unstable in solution and slowly revert to the Mn^{III} derivative [80], a process accelerated by white light. The first-order rate constant for spontaneous reduction in air at 25°C, pH 13 aqueous solution, is 2.5×10^{-6} sec^{-1}. The apparent heat of activation was found to be 20 kcal/mole and an activation entropy −25 cal/mole.deg was calculated; the reaction rate is independent of added anion but is accelerated by a factor of ten in the

absence of air and is enhanced as the pH is decreased. The oxidation product formed in the reduction of the Mn^{IV} porphyrin is still open to question. The oxidation of water to form hydrogen peroxide or oxygen was ruled out, since neither of these products was observed. Evidence from infrared spectra indicate that the product is an oxidation product of the carboxylic acid side chain (percarboxylic acid or diacetylperoxide) [80]. Addition of excess ferrocyanide to Mn^{IV} porphyrins yields a spectrally distinct material which has been tentatively designated as Mn^{V} porphyrin [10]. The evidence for the existence of Mn^{IV} porphyrins is not altogether compelling. In addition to metal oxidation, it is possible to oxidize the porphyrin, i.e. remove an electron from a π orbital and form a porphyrin radical. This has been shown for a number of metalloporphyrins using a combination of controlled electrolysis in aprotic solvents with visible and ESR spectroscopy [81]. Before the existence of Mn^{IV} porphyrins can be conclusively shown, measurements of this sort must be made for Mn^{III} porphyrins.

E. MANGANESE PORPHYRIN–PROTEIN COMPLEXES

A number of Mn porphyrins have been incorporated into a series of apoproteins that normally bind hemes. In general, the heme group is removed by the acid–butanone extraction of an aqueous phase of the hemeprotein. The separated aqueous solution of the apoprotein is then mixed with an aqueous solution of an Mn^{III} porphyrin [82]. The complex is purified by column chromatography. The apoprotein binds one Mn^{III} porphyrin for every heme group that is bound in the naturally occurring heme protein [24]. The binding presumably occurs at the same site, without gross changes in the protein conformation [83]. Table 4 lists the complexes reported to date.

The absorption spectra of the Mn^{III} porphyrin protein complexes have been recorded and the absorption maxima tabulated [24]. Although the spectral pattern is preserved, there is a small red shift ($\sim$ 0.3 kK) in going from the aqueous solution spectrum of the Mn^{III} porphyrin to the aqueous solution spectrum of the protein complex. This shift may be related to a change in the dielectric medium around the Mn^{III} porphyrin, i.e. from the high dielectric constant environment of water to the low dielectric medium inside the hydrophobic region of the protein. While the spectra of Mn^{III} porphyrins are equivalent for the CCP and HRP complexes, those of MB are appreciably blue shifted, which may indicate an environmental difference at the protein binding site. This effect is not unlike the solvent shift noted above. Addition of N_3^-, F^- and CN^- to the protein complexes does not alter the absorption spectrum of the MB or HRP complexes, indicating that these ions do not bind. On the other hand, spectrally distinct complexes of F^- and N_3^- appear to be formed with the CCP derivative. This result is in marked contrast to the lack of binding in aqueous solution for the free Mn^{III} porphyrin. The question remains as to how the Mn^{III} porphyrin is bound to the apoprotein. One of the axial coordination positions of the metal is most likely filled by a hydroxide ion. The other position may be filled by an imidazole group of a histidine residue from the protein, as is the case for the naturally occurring hemeproteins [2,3]. Although magnetic susceptibility measurements have not been made on the protein derivatives, the absorption spectra are typical for high-spin d^4 Mn^{III} porphyrins. As with the free Mn^{III} porphyrin, no ESR signal is observed for the protein complexes that can be assigned to the metal ion.

TABLE 4

Reconstituted manganese(III) porphyrin protein complexes

Complex	Apoprotein		Biological activity	Ref.
[Mn(Prpor)(OH)H_2O]	Apocytochrome b_5	CYT	None	84
[Mn(Mesopor)(OH)H_2O]		CYT	Not investigated	84
[Mn(Mesopor)(OH)H_2O]	Apohemoglobin	HB	Not investigated	83
[Mn(Prpor)(OH)H_2O]		HB	None	85
[Mn(Prpor)(OH)H_2O]	Apomyoglobin	MB	None	24
[Mn(Hpor)(OH)H_2O]		MB	None	24
[Mn(Depor)(OH)H_2O]		MB	None	24
[Mn(Mesopor)(OH)H_2O]		MB	None	24
[Mn(Prpor)(OH)H_2O]	Apocytochrome c peroxidase	CCP	Some	82, 24
[Mn(Depor)(OH)H_2O]		CCP	Some	24
[Mn(Mesopor)(OH)H_2O]		CCP	Some	24
[Mn(Hpor)(OH)H_2O]		CCP	Some	24
[Mn(Mesopor)(OH)H_2O]	Apohorseradish peroxidase	HRP	Some	24
[Mn(Prpor)(OH)H_2O]		HRP	Some	24
[Mn(Depor)OH)H_2O]		HRP	Some	24
[Mn(Hpor)(OH)H_2O]		HRP	Some	24

The Mn^{II} porphyrin protein complexes can be generated in situ by addition of $Na_2S_2O_4$ to the appropriate solution of the Mn^{III} derivative [24]. The absorption spectra are typical of Mn^{II} porphyrins. ESR spectra of the complexes of [Mn(Prpor)H_2O] with HRP, MB, HB and CCP have been measured in frozen aqueous solution, pH 7, at 77°K. The spectra are typical of a high-spin tetragonal Mn^{II} complex. The x-band spectra show two prominent signals at $g_\perp = 5.9$ and $g_\parallel = 2.0$ with Mn^{II} nuclear hyperfine lines, $A_\perp = 0.0073$ cm^{-1} and $A_\parallel = 0.011$ cm^{-1}. In a few cases, more than the six expected metal hyperfine lines are seen, the additional lines arising because of rhombic distortion. Ligand nitrogen ($I=1$) superhyperfine splittings have not been observed for either the free Mn^{II} porphyrins or the protein complexes. Analysis of the spectra yields the zero field parameters D and $\lambda(E/D)$. The D values for the protein complexes are ~ 0.5 cm^{-1}, which indicates a very small axial distortion in the Mn^{II} porphyrins. In fact, the axial distortion is an order of magnitude smaller than for the isoelectronic Fe^{III} porphyrin. Although somewhat better resolved, the ESR spectra of the Mn^{II} porphyrin protein complexes are very similar to those of the free Mn^{II} porphyrins. A small rhombic distortion, $E/D \approx 0.02$–0.002, is also indicated by the ESR spectra. The extent of the x, y distortion in the Mn^{II} porphyrins seems to depend on the protein and is greatest for CCP and least for HRP.

The Mn porphyrin protein complexes have been tested for biological activity. The biological function of cytochrome b_5 is as a component of an electron transfer chain in animal chromosomes. Apparently the Mn^{III} porphyrin does not have the proper redox potential

to show biological activity [84]. In the case of the myoglobin and hemoglobin derivatives, the biological activity was measured with the Mn^{II} porphyrin derivatives; since the Mn^{II} complexes do not bind oxygen or carbon monoxide, they show no biological activity [24,85] Nevertheless, it is interesting to note that a manganese porphyrin has been found in small quantities in human blood [86]. A function of naturally occurring peroxidases is to catalyze the decomposition of hydrogen peroxide. An intermediate in this process is thought to be an Fe^{IV} porphyrin [24], and the Mn^{III} porphyrin derivatives of both CCP and HRP show partial activity in these enzymic reactions [24]. The manganese complexes were found to react with one molecule of H_2O_2 per Mn^{III} porphyrin to form a "peroxide" complex, the rate of formation being more than three orders of magnitude slower than the corresponding hemeprotein. This material is spectrally different for HRP and for CCP and is thought to contain higher oxidation states of manganese. In the case of CCP, the complex is two oxidizing equivalents higher than an Mn^{III} porphyrin. The exact nature of these higher oxidation states is not known. However, the absorption spectra are similar to the "Mn^{IV}" porphyrin previously reported. The complexes show no ESR signal that can be assigned to the complex and the magnetic moments of the materials remain to be measured. Both peroxide complexes catalyze the peroxidatic oxidation of ferrocytochrome c several orders of magnitude slower than the hemeproteins.

Physical and chemical properties of the Mn porphyrin proteins indicate that there are no gross changes in the Mn porphyrins when the complex is incorporated into the apoprotein. However, the small differences noted above make these materials attractive for further detailed study.

F. MANGANESE CHLOROPHYLLS

Several complexes of Mn^{III} and a chlorophyll-like ligand have been reported: [Mn(pheophytin$_a$)(OH)H_2O] [87], [Mn(Mepheo$_a$)(Cl)H_2O] [89] and [Mn(chlorin e_6)($C_2H_3O_3$)H_2O] [88]. Structural representations are given in Fig. 9. The complexes can be

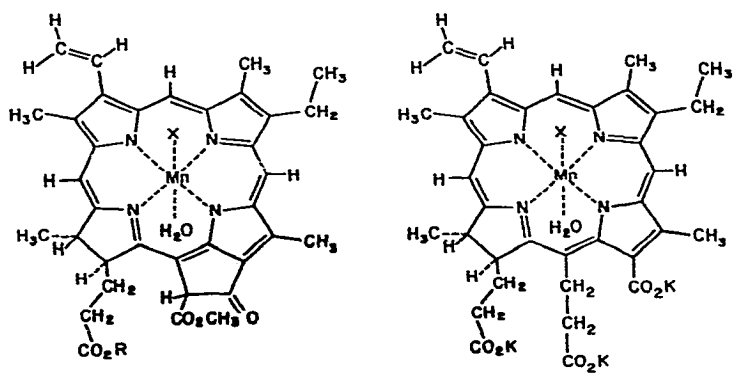

Fig. 9. Structural representation of Mn^{III} chlorophylls: figure on left, R = CH_3, methylpheophorbide$_a$; R = $C_{20}H_{39}$, pheophytin$_a$; figure on right, potassium chlorin e_6.

easily prepared by the general synthetic method. [Mn(Mepheo$_a$)(Cl)H$_2$O] is paramagnetic with a magnetic moment of 4.76 B.M., consistent with high-spin d^4 Mn^{III}. Only the visible absorption spectra of the Mn^{III} chlorophylls have been recorded and these are typical of that of a chlorin and a high-spin Mn^{III} complex. In a chlorin, two of the β ring positions of the porphyrin are reduced and, as a result, the highest filled and lowest empty πM.O. of the macrocycle are altered. The filled a_{2u}, a_{1u} levels are no longer accidentally degenerate; the a_{2u} level remains at the same energy while the a_{1u} is raised in energy. Further, the doubly degenerate empty e_g^* level is split, giving one level of slightly higher energy and another at still higher energy. Transitions among the four orbitals give rise to a strong Q_y band at low energy, a weak Q_x band at an energy comparable to the porphyrin case, and two closely spaced B_x, B_y bands at higher energy, again comparable to that of the porphyrins. Although perturbed by the special Mn^{III} interaction, these features are seen in Fig. 10 which displays the spectrum of [Mn(Mepheo$_a$)(Cl)H$_2$O]. In methanol solution [34], band IV is identified with the strong Q_y band at 14.9 kK and band III may be a weaker absorption at ~18.5 kK. The first of these is red-shifted by ~3 kK from the porphyrin case. Band VI at 26.9 kK which can be identified with B_x, B_y transitions is broadened and blue-shifted from the band for divalent metallochlorins [90]. Although its intensity is somewhat low, band V appears at approximately the same energy, 21.3 kK, as in the porphyrin case. On the other hand, the weak bands I and II at 9.7 and 11.1 kK are considerably red-shifted (~3 kK) and weakened. This is in agreement with the notion that the highest filled π molecular orbital has been destabilized in the chlorins. All the features indicate that the Mn^{III}–chlorophyll π mixing is present in these complexes. However, the relatively low intensity of the charge-transfer bands may be a consequence of a lowering of the ligand π character in the metal $d\pi$ orbital. This difference may be a consequence of several factors. Destabilization of the e_g^* levels in the chlorin would decrease the metal–ligand π mixing, and a non-planar structure would lead to less efficient sigma donation and π acceptor ability of the chlorin ligand. The visible spectra of [Mn(Mepheo$_a$)(Cl)H$_2$O] in pyridine, glacial acetic acid, 20% H$_2$O–ethanol and of [Mn(pheophytin$_a$)(OH)H$_2$O] in ethanol have been recorded. The display is similar to that of [Mn(Mepheo$_a$)(Cl)H$_2$O]. The spectra of [Mn(chlorin e_6)(C$_2$H$_3$O$_2$)H$_2$O] in water and 2M sodium hydroxide are considerably different [88]. The maxima blue shift by ~1 kK when the hydroxide complex is formed.

$$[\text{Mn(chlorin } e_6)(\text{OH})\text{H}_2\text{O}] + \text{OH}^- \rightarrow [\text{Mn(chlorin } e_6)(\text{OH})_2]^- + \text{H}_2\text{O} \qquad (18)$$

The only property related to axial ligation of the manganese chlorophyll derivative that has been measured [73] is

$$[\text{Mn(Mepheo}_a)(\text{Cl})\text{H}_2\text{O}] + 2\,\text{S}_4\text{O}_4^{2-} \rightleftarrows [\text{Mn(Mepheo}_a)(\text{S}_2\text{O}_4)]_2^{3-} + \text{Cl}^- + \text{H}_2\text{O} \qquad (19)$$

The binding constant in ethanol is $K_2 = 4 \times 10^7$. Presumably the weak in-plane chlorophyll donor here allows a strong axial interaction.

Mn^{III} chlorophylls can be reduced to the Mn^{II} derivatives by addition of $Na_2S_2O_4$ to a basic solution of pyridine–water or ethanol–water [88]. Similarly, reduction of ethanol solutions with a hydrogen–palladium black or of aqueous solutions with Na_2S or $Na_2S_2O_3$

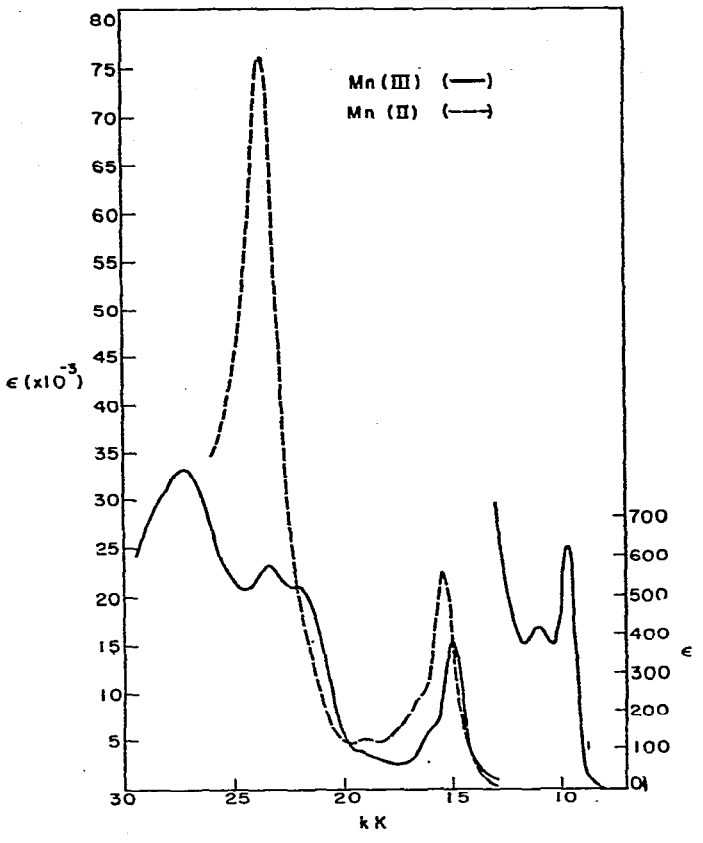

Fig. 10. Absorption spectra of chloro(aquo)methylpheophorbide$_a$manganese(III) in ethanol–water, pH 11 with $Na_2S_2O_4$ added (- - -) and without $Na_2S_2O_4$ (——).

have been carried out [87,89]. The materials are rapidly oxidized in the presence of air. The spectra of the reduced solutions (Fig. 10) show the normal metallochlorin spectrum suggesting that the Mn^{II} complexes are very similar to the other divalent metal complexes [90]. As expected, band V is gone, the Soret band appears in the lower energy region and band IV moves to higher energy. Thus, the Mn^{II} chlorophylls do not show any indication of a strong metal–ligand π mixing.

The potentials for the reduction of $Mn^{III} \rightarrow Mn^{II}$ have been measured polarographically and potentiometrically for [Mn(Mepheo$_a$)(Cl)H_2O] in non-aqueous and aqueous solution (see Table 3). The potentials are 0.1–0.2 V more positive than for the porphyrin complexes, in agreement with the presumed weaker donor strength of the chlorophylls. Over a narrow range (7.8–10.0) the potential is independent of pH in aqueous solution. Surprisingly, the ligand reduction potential for [Mn(Mepheo$_a$)H_2O] in acetonitrile is 0.28 V more positive than for [Mn(DMPrpor)H_2O]. The molecular orbital model for chlorin predicts that both e_g^* levels will be destabilized and thus the addition of an electron to the

levels should be more difficult than for the porphyrins. Perhaps the anomaly here can be explained by noting that this may be a substituent effect, i.e. that the comparison is made between a system with an exocyclic ring and one without.

Solutions of the Mn^{III} chlorophylls can be reduced in the absence of air by irradiation with visible light, the product in all cases being the Mn^{II} chlorophyll and only a small amount (>10%) of the pigment is destroyed during the process. Reoxidation occurs in the dark and in air. Ultraviolet irradiation has little reducing power. The kinetics of photoreduction, in aqueous ethanol pH 9, of [Mn(Mepheo$_a$)(Cl)H_2O] yields [73] the first-order rate constant 3.7×10^{-4} sec^{-1}. This is a comparable value to that found for Mn^{III} porphyrin photoreduction. The photoreduction of [Mn(pheophytin$_a$)(OH)H_2O] in ethanol has also been observed [87]. The reaction is more rapid in aqueous ethanol. The oxidation product has been identified as acetaldehyde which is formed from ethanol. The photoreduction of [Mn(chlorin e_6)($C_2H_3O_2$)H_2O] has been investigated in somewhat more thorough fashion [88], the reaction proceeding quite readily in 2*M* sodium hydroxide solution. The quantum yields are rather small, being 1.3×10^{-5} in the red region and 5×10^{-5} in the blue region of the spectrum. The quantum yield drops off rapidly as the hydroxide ion concentration is decreased. Presumably the photoactive complex in this system is [Mn(chlorin e_6)$(OH)_2]^-$ and the oxidation product here appears to be hydrogen peroxide. Under optimum conditions, the yield of the hydrogen peroxide formed in the photoreduction reaches 57% of the stoichiometric amount. More detailed work is obviously needed on these very interesting systems.

The oxidation of [Mn(Mepheo$_a$)(OH)H_2O] by sodium hypochlorite in aqueous solution, pH 13, has been briefly studied [73]. The spectrum of the oxidized complex, tentatively identified as [Mn(Mepheo$_a$)$(OH)_2$], does not show any band V and resembles a normal metallochlorin spectrum. The potential for the oxidation of $Mn^{III} \rightarrow Mn^{IV}$ is estimated to be +0.41 V at pH 12 and +0.36 V at pH 13. This value is a little (0.02 V) more positive than for [Mn(Hpor)(OH)H_2O] and this is in qualitative agreement with the notion that the weaker donor chlorophyll complex should be more difficult to oxidize. Autoreduction of Mn^{IV} chlorophyll complexes also takes place slowly.

G. MANGANESE PHTHALOCYANINES

Much of the work on manganese porphyrin complexes was prompted by some observations of Elvidge and Lever about phthalocyanine complexes [91]. Therefore it is appropriate to discuss these materials briefly here and to contrast their behavior with that of the porphyrin complexes. Although it is generally thought that metallophthalocyanine and metalloporphyrins show closely similar behavior, there are many important differences which are exhibited in a striking fashion by the manganese complexes. A recent review by Lever is recommended for a detailed discussion of the phthalocyanines [92].

Mn^{II} phthalocyanine can be prepared by the condensation reaction of phthalonitrile and manganese dioxide or manganese acetate [92], the complex [Mn(PC)] being purified by vacuum sublimation. The crystals formed contain a four-coordinate square planar Mn^{II} complex [93] with a magnetic moment, $\mu = 4.33$ B.M. at 20°C, which corresponds to three unpaired electrons and a metal orbital population of $b_{2g}^2 e_g^2 a_{1g}^1$ (ref. 94). In the presence of pyridine (and the absence of air) the complex picks up two pyridine molecules

to form the octahedral complex $[Mn(PC)Py_2]$. The electron spin resonance spectrum of this material at 90°K in frozen pyridine [73] (and absence of air) is consistent with a spin ½ system and a metal d orbital population of $e_g^4 b_{2g}^1$. The ESR parameters are $g_{\|} = 1.90$, $g_{\perp} = 2.16$, $g_0 = 2.07$, $A_{\|} = 151 \times 10^{-4}$ cm^{-1} and $A_{\perp}$, 25×10^{-4} cm^{-1}. The temperature dependence of the solution absorption spectrum of $[Mn(PC)Py_2]$ may indicate that in the temperature range 20 to 90°C, the compound is a mixture of spin states ($S = ½$ and $S = {}^3/_2$) [95]. The complex 4, 4′, 4″, 4‴ sulfophthalocyanine manganese(II) [96], [Mn(SPC)], has been prepared and it has a magnetic moment analogous to that of [Mn(PC)]. In aqueous solution, the magnetic moment drops to that expected for a spin-paired Mn^{II} complex. This may be ascribed to axial binding by water molecules but it seems more likely that this is a reflection of oxidation of the material. The salt $Na[Mn(PC)(C_2H_5OH)CN]$ can be prepared in a saturated solution of sodium cyanide in ethanol in a nitrogen atmosphere [26]. The absorption spectrum of [Mn(PC)], which is not typical of divalent metallophthalocyanines, undergoes a blue shift when $[Mn(PC)Py_2]$ is formed. Both spectra show additional absorption in the near IR at 10 and 12 kK as well as a strong band at ~22 kK in addition to the normal $\pi \rightarrow \pi^*$ bands at ~15 kK and ~30 kK. Whether this is an indication of a ligand–metal π mixing in these complexes is not known. It is worthwhile noting that the low-spin $[Mn(PC)Py_2]$ complex with the filled $d\pi$ level should be a good π donor to the empty phthalocyanine π^* orbitals. Chemical reduction of [Mn(PC)] with lithiumbenzophenone in tetrahydrofuran (THF) yields one- and two-electron reduction products, $[Mn(PC)(THF)_2]^-$ and $[Mn(PC)(THF)_2]^{2-}$ (ref. 97). Magnetic moments of the materials yield two and three unpaired electrons for the complexes respectively. These values are consistent if the complexes are formulated as low-spin complexes of Mn^{II} with the one- and two-electron reduction product of the phthalocyanine ligand.

Exposure of air to a methanol solution of [Mn(PC)] quickly leads to air oxidation [26].

$$[Mn(PC)(MeOH)_2] \xrightarrow{[O_2]} [Mn(PC)(OH)MeOH] \qquad (20)$$

The analogous ethanol complex can also be prepared. Addition of HCl to the latter material gives the corresponding chloride complex. Undoubtedly, many other anion complexes of this type can be formed by adding the appropriate salt of the anion to the methanolic solution. Addition of excess NaCN and NaOH to these solutions gives $[Mn(PC)(CN)_2]^-$ and $[Mn(PC)(OH)_2]^-$. Air oxidation similar to the one carried out in methanol can be performed in glacial acetic acid to give $[Mn(PC)(C_2H_3O_2)C_2H_4O_2]$ [26]. In pyridine with added HCl or acetic acid, the materials isolated are $[Mn(PC)(C_2H_3O_2)Py]$ and [Mn(PC)(Cl)Py]. In the absence of added anion, the dimer is formed [25].

$$2[Mn(PC)Py_2] \xrightarrow{[O_2]} [Mn(PC)_2(Py)_2O] \qquad (21)$$

The monomer hydroxide complex is undoubtedly an intermediate in the dimerization reaction. The compositions of all the complexes formed are consistent with six-coordinate complexes of Mn^{III}. The room-temperature magnetic moments of solid $[Mn(PC)(OH)(CH_3OH)]$ and $[Mn(PC)(C_2H_2O_2)Py]$ are 4.87 B.M. and 4.76 B.M., corresponding to a high-spin d^4 Mn^{III} complex [26]; presumably the other monomeric monoanion complexes

show similar moments. The magnetic moments of the dicyano and dihydroxo complexes have not been determined. It is interesting to note that Mn^{III} phthalocyanines are one of the rare examples known of high-spin metallophthalocyanines with more than $3d$ electrons [92]. Apparently, spin pairing of Mn^{III} complexes does not readily occur. The magnetic susceptibility of the dimer $[Mn_2(PC)_2(Py)_2O]$ yields values of ca. 2 B.M. at room temperature [24], the moment decreasing to ~1.3 B.M. at 77°K. The low moment probably results through superexchange of the two high-spin Mn^{III} ions across the bridging oxygen atom. Of course, a similar process could also occur if the Mn^{III} was an intermediate spin case. The crystal and molecular structure of the dimer has recently been determined [98] and shows the Mn^{III} atom in the plane of the planar phthalocyanine with one axial bond to a pyridine molecule and the other to an oxygen atom which forms a linear Mn—O—Mn bridge. The Mn—N (phthalocyanine) distance is 1.97 Å and the Mn—N (pyridine) distance is 2.15 Å. The in-plane bond distance is ~0.03 Å shorter than for the [Mn(TPP)Cl]. This is a typical bond shortening in going from porphyrins to phthalocyanines [28]. The axial bond to oxygen, 1.71 Å, is shorter than the sum of the ionic radii. It would thus appear that the manganese forms one strong and one weak axial bond. The molecular structures of the other Mn^{III} phthalocyanines are not yet known and it will be of some interest to know if these complexes are in plane as the dimer or out of plane.

As expected, the Mn^{III} phthalocyanines show no observable ESR signal at x-band frequencies. Although many spectra have been recorded, no systematic study of the electronic spectra of Mn^{III} phthalocyanines has been reported. Qualitatively, the absorption spectra show near IR bands at 9 and 10 kK as well as an additional band at ~19 kK and the normal $\pi \rightarrow \pi^*$ absorptions; additional features appearing in the spectra may arise from an Mn^{III}—porphyrin π mixing. The spectrum of the dimer in pyridine is quite different from that of the monomeric complex and it seems therefore that the spectra are sensitive to the axial ligands. For example, the formation of $Na[Mn(PC)(CN)_2]^-$ in MeOH from [Mn(PC)(OH)MeOH] gives rise to a blue shift of ~1 kK.

The kinetics of dimer formation in aqueous solution at 25°C have been worked out for $[Mn(SPC)(OH)H_2O]$ [99].

$$[Mn(SPC)(OH)_2]^{5-} + [Mn(SPC)(OH)H_2O]^{4-} \underset{k_3}{\overset{k_1}{\rightleftharpoons}} [Mn_2(SPC)_2(H_2O)(OH)(OH)O]^{9-} + H_2O \quad (22)$$

$$2[Mn(SPC)(OH)H_2O] \overset{k_2}{\rightarrow} [Mn_2(SPC)_2(H_2O)_2O]^{8-} + H_2O \quad (23)$$

At pH 11, $k_1 = 8.3 \times 10^2 M^{-1}.sec^{-1}$ and at pH 12, $k_2 = 1.2 \times 10^2 M^{-1}.sec^{-1}$, $k_3 = 7.0 \times 10^{-4}$ sec^{-1}. No intimate mechanism for this complicated reaction has been proposed. Mn^{III} phthalocyanines can be photoreduced to the Mn^{II} complexes in the absence of air in pyridine solution [26]. The presence of pyridine appears to be necessary for photoreduction since solutions in ethanol, methanol and chloronaphthalene show no reaction. Far-red light is most active in the reaction. The polarographic reduction [100] of $[Mn_2(PC)_2(Py)_2O]$ in pyridine gave a wave at ~0.64 V, which presumably refers to the $Mn^{III} \rightarrow Mn^{II}$ reduction. Finally, sublimation of Mn^{III} phthalocyanines in the absence of air leads to spontaneous vapor-phase reduction to the Mn^{II} derivative. The magnetic properties of several high-spin Mn^{IV} phthalocyanines have been reported [101].

The major difference between the Mn^{II} phthalocyanines and porphyrins are *(1)* the phthalocyanine forms an intermediate-spin four-coordinate planar complex whilst the porphyrin is a high-spin complex that is most likely five-coordinate and non-planar; *(2)* in the presence of donor molecules like pyridine, the phthalocyanines form a spin-paired (low-spin) six-coordinate complex whilst the porphyrin forms a six-coordinate spin-free complex (high-spin). The ability of the phthalocyanine to cause metal *d* electron spin pairing is general and may be related to its strong ligand field. Spin pairing by axial ligation also points up the rather stronger axial interaction in the phthalocyanine complexes than for the porphyrins. Although Mn^{II} phthalocyanines are among the less stable divalent metallophthalocyanines, concentrated sulfuric acid is needed for demetallation. In contrast, dilute acid quickly demetallates Mn^{II} porphyrins. This difference is probably related to the low-spin in-plane structure of the phthalocyanines and the high-spin out-of-plane structure of the porphyrin complex.

The overall behavior of Mn^{III} porphyrins and phthalocyanines is similar, both forming six-coordinate high-spin complexes. In detail, though, the two systems differ in their axial coordinating ability. The property appears to be stronger for the phthalocyanine than for the porphyrin. This is shown by the ability of the former to form solvates, dianion complexes and dimeric complexes, which complexes are not noted with the porphyrin and may arise naturally from a difference in molecular structure, viz. metal in-plane versus out-of-plane. Further, the reduction potential for $[Mn_2(PC)_2(Py)_2O]$ is about 0.3 V more negative than for the strongest porphyrin donor. This indicates a considerable increase in stabilization of the higher oxidation state for the phthalocyanine over the porphyrin which is in line with the greater donor strength of phthalocyanines.

H. COMPARISON WITH IRON PORPHYRINS

Superficially, the coordination chemistry of Mn and Fe porphyrins appears to be similar. There are, however, many important differences which lead to a biological differentiation of the two transition elements. A brief discussion of these seems appropriate here to point out the special features of Mn porphyrins. In air, Fe^{III} porphyrins are the most stable oxidation state of the metal. The complexes can adopt two molecular structures, each with its particular spin state: an out-of-plane five-coordinate high-spin complex [65] and an in-plane six-coordinate low-spin complex [102]. The change in structure is related to the strength of the axial ligands; spin pairing occurs with good nitrogen base donors and cyanide ion. In general, relatively strong axial binding is a feature of the iron porphyrins, the FeCl distance in [Fe(TPP)Cl] [65], for example, being considerably shorter than the sum of the ionic radii. On the other hand, the absence of a low-spin form of Mn^{III} porphyrins and a weak axial interaction seem to be a feature of their chemistry. The stronger axial binding in the Fe^{III} porphyrins is illustrated by the higher binding constant for pyridine [27] and by the lower pK_a of the aquo ligand [31] when compared to Mn^{III} porphyrins.

High-spin Fe^{III} porphyrin complexes show characteristic weak near-IR absorption bands. These have been assigned to porphyrin π to metal $d\pi$ transitions. The position of the maxima is very sensitive to the axial ligand with a spread of more than 2.5 kK in going from the methoxide ligand to the iodide for [Fe(DMDepor)X] [103,104]. Although

the same ligand order is observed for Mn^{III} derivatives, the energy interval here is only one-fourth as large. Many other properties of Fe^{III} porphyrins are sensitive to the axial ligand (e.g., Mössbauer spectra, zero field splitting [104]). The sensitivity of the axial interaction for Fe^{III}, in comparison to Mn^{III}, may be related to the molecular structure of high-spin Fe^{III} porphyrins. With Fe^{III} considerably out of the porphyrin plane toward the axial anion, the iron atom can bind in a fairly specific way to the axial anion. Strong interactions with the porphyrin ligand are lessened by the placement of the metal out of the plane. In contrast to this, in Mn^{III} porphyrins the metal atom is considerably closer to an in-plane structure and axial binding is weak.

The extent of the Fe^{III}–porphyrin interaction can be assessed by examining absorption spectra. The complexes do not show intense charge transfer bands in the 20–22 kK region as do the Mn^{III} porphyrins [56]. Of course, weak absorptions are seen in this region and the broadened α, β bands indicate several other unresolved absorption maxima. In support of this MCD spectra do show several additional features here [53]. Further, the near-IR charge transfer bands of Fe^{III} porphyrins are relatively weak. The intense nature of the charge-transfer bands for Mn^{III} porphyrins has been related to strong porphyrin–metal π mixing. The absence of a strong visible charge-transfer band and the weak near-IR bands may be taken as evidence for a much weaker π interaction in the Fe^{III} porphyrins. Nevertheless, the difference in the spectra of the Mn^{III} with Fe^{III} porphyrins is one of degree, not of kind. In fact, the assignment scheme given here for the Mn^{III} porphyrins can apply equally well to the spectra of the Fe^{III} porphyrins. The fact that the latter materials show a normal Soret band indicates that the coupling of the ligand and charge-transfer bands that gives rise to band VI in the Mn^{III} porphyrins is absent in the Fe^{III} porphyrins. This is consistent with the expected stabilization of the Fe^{III} d orbitals which removes the accidental degeneracy of the two transitions.

The difference in π bonding behavior between Fe^{III} and Mn^{III} porphyrins may be due to the stability of the metal d orbitals. The charge transfer bands of the high-spin Fe^{III} porphyrins are red-shifted from those of the Mn^{III} porphyrins. This is consistent with an increasing stability of the d orbitals in going from Mn^{III} to Fe^{III}. This change in energy increases the energy mismatch between the metal $d\pi$ and porphyrin e_g^* level and this would lower the π interaction. An additional point relating to molecular structure and d-orbital population is relevant here. High-spin Fe^{III} differs from Mn^{III} in that the latter has an electron in the $d_{x^2-y^2}$ orbital, which orbital is strongly σ antibonding with respect to the porphyrin. The energy of the orbital can be depressed somewhat if the iron atom is out of the plane of the porphyrin; the farther out, the lower the energy [57]. The Fe^{III}, of course, adopts a configuration which represents a balance of σ and π in-plane and out-of-plane interactions. The exaggerated square pyramidal structure for Fe^{III} porphyrins places the metal atom in a less favorable position for π overlap. Since the $d_{x^2-y^2}$ orbital is not occupied for Mn^{III}, the above restriction is not imposed on its complexes.

In addition to the trivalent ions, the divalent metalloporphyrins exhibit substantial differences in behavior. The Fe^{II} porphyrins are thought to adopt two molecular structures, each with its peculiar spin state. One is an in-plane six-coordinate low-spin complex and the other is a high-spin presumably five-coordinate and out-of-plane complex [3]. The low-spin form is quite readily formed in the presence of good donors. In contrast to this, Mn^{II} porphyrins only form high-spin complexes; i.e. spin pairing is not noted. The relative ease

of spin pairing in Fe porphyrins may be related to the increase in nuclear charge. Axial ligation is also stronger in Fe^{II} porphyrins than in Mn^{II} porphyrins [33]. It is interesting to note that low-spin Fe^{II} would be a good π donor since its $d\pi$ orbitals are completely occupied; not only are porphyrin π interactions possible here but axial π donation can also be invoked [56]. Nevertheless, spectral properties of both Mn^{II} and Fe^{II} porphyrins indicate a lack of metal porphyrin π interaction.

The difference in electronic structure is also reflected in the redox properties of the materials. For example, in aqueous solutions [Fe(Prpor)(OH)H_2O] is more easily reduced than [Mn(Hpor)(OH)H_2O]; i.e. the potential is 0.03–0.05 V more positive [105]. The increased stability of Mn^{III} over Fe^{III} may be related to the stronger porphyrin interaction in the former complex. As expected, the rate of reduction of Fe^{III} porphyrins is somewhat more rapid than that of Mn^{III} porphyrins [71]. In this case, aside from the additional electron, there appears to be no spin state change in the reduction. Conversely, when strong axial ligands such as pyridine are present with Fe^{III} porphyrins, the reduction involves low-spin complexes where the stability of Fe^{III} oxidation state is lowered considerably. On the other hand, the pyridine complexes of Mn^{III} and Mn^{II} porphyrins are both high-spin. The stability of the Fe^{III} with respect to Mn^{III} is then reduced for $[M(Hpor)Py_2]^{2+}$; the reduction potential is ~0.38 V more positive for Fe (ref. 106).

Attempts to show biological activity by replacing the heme in a hemeprotein by Mn porphyrins have met with mixed success. For those biological functions that involve the lower oxidation state of the metal, no biological activity was found for the Mn complexes. For example, cytochrome b_5 activity involves precisely fitting a particular redox potential into a chain of electron transfers. The redox potential can change greatly if a spin state change is involved for Fe porphyrins. The Mn^{III} is, of course, restricted in this respect. The biological function of myoglobin and hemoglobin involves the transport of molecular oxygen via axial bonding to the low spin Fe^{II} porphyrin. This configuration is required to give oxygen binding. Since no low spin forms of Mn^{II} porphyrins are known, it is not surprising that the Mn^{II} porphyrin proteins do not show any biological activity (do not bind oxygen). Conversely, in those biological processes like peroxidase activity that involve Fe^{III} and its higher oxidation states, Mn^{III} porphyrins show some activity. This suggests that the oxidation potentials of Fe^{III} and Mn^{III} porphyrins are not greatly different and also that Fe^{IV} and Mn^{IV} may be similar in properties and structure [107].

I. MODEL COMPOUND STUDIES

In green-plant photosynthesis, several transition elements are needed for normal function of the chloroplast [108]. One of these, manganese, is required for the oxygen evolution [6]. The photochemical splitting of water into a reducing function and oxygen occurs in a part of the photosynthetic unit called photosystem II [108]. Several investigations have suggested, on the basis of photochemical experiments, that the manganese is involved in the oxidant side of photosystem II [109]. The absorption of radiant energy by the mass of chlorophyll a molecules of photosystem II results in the ejection of an electron from a reaction center chlorophyll a [109], which electron is eventually utilized in the reduction of carbon dioxide. The reaction center chlorophyll a molecule cation is now a powerful oxi-

dizing agent and it abstracts an electron from another species. This latter material may be an Mn complex [5]. The electron transfer could form a complex of Mn in a high oxidation state which would be a powerful enough oxidizing agent to oxidize water (and form oxygen). Of course, this is a rather simple model and other compounds may be involved in the process, acting as components in the electron transfer chain from water to the reaction center chlorophyll a. Further, Mn may not be directly involved in the oxidation of water but may react with an intermediate oxidation product between water and oxygen. Finally, it may be involved in both! There appear to be three manganese atoms per photosystem II center: two of one kind at one site, one of another at a second site [109]. The metal atoms are physically located in the membrane protein portion of the chloroplast and the manganese is difficult to remove unless the membrane structure is disrupted and the protein is denatured. The manganese complex does not appear to be a special chlorophyll molecule associated with chlorophyll in the lipid phase but the evidence does not rule out a similar complex contained in the protein phase. As yet, the active manganese complexes have not been isolated from the chloroplast. Further, no physical or spectral property of the metal can be observed in vivo. Thus the ligand atoms binding the metal well as the metal oxidation states are not known. Recent work has shown that O_2 evolution requires several activating light flashes [109] which suggests that some photooxidation must occur and may be related to the formation of a high oxidation state of manganese.

The role that manganese plays in the photosynthetic liberation of oxygen from water is undoubtedly linked to the ability of the metal ion to function as a redox catalyst [8]. The utility of the metal ion in this process depends on the potential resulting from the changes between the oxidation states and the availability of suitable oxidation states. Both of these are a function of the ligand field around the metal ions [70]. Although the binding site of manganese in the photosynthetic unit has not been assigned, the donor atoms surrounding the metal will most likely be nitrogen or oxygen (or less likely, sulfur) of a prosthetic group or of an apoprotein. The ligand field may be composed of all of one kind of donor atoms or a mixture of several kinds. Good model ligands for the nitrogen donor prosthetic group are porphyrins. In addition to being peripatetic biological ligands, they form complexes with Mn^{II}, Mn^{III} and Mn^{IV} (ref. 8). Although the coordination chemistry, redox chemistry and photoreduction of Mn^{III} and Mn^{II} porphyrins are fairly well characterized and understood, the Mn^{IV} complexes have not been characterized in detail. At any rate, the bulk of the work yet to be done on manganese porphyrins will involve the higher oxidation materials, presumably Mn^{IV}. In this context, the work on the manganese porphyrin analogs of cytochrome c peroxidase and horseradish peroxidase will be particularly relevant.

Lest the importance of manganese porphyrins as model compounds be overstressed, several other model systems also suggest themselves. For example, a likely manganese complex in the chloroplast could involve direct binding of the metal to a protein or to a flavin, i.e. nitrogen–oxygen donors. Good models for both of these systems would be Schiff base complexes. The report that an Mn^{III} complex of pyridoxal and alanine catalyzed the reversible reduction of oxygen to form hydrogen peroxide may be significant in this context[110]. Aqueous solutions of Mn^{III} as well as complexes of oxygen donors are quite potent oxidizing agents [69]. In fact, Mn^{III} in water rapidly decomposes hydrogen peroxide to give molecular oxygen [69]. Therefore, many other Mn model systems are likely to have biological

relevance as do the porphyrin complexes. Unfortunately, the coordination chemistry of Mn is not far advanced. Perhaps the future will see an increase of both our knowledge of manganese chemistry and also of its role in photosynthesis.

NOTE ADDED IN PROOF

The synthesis in 0.05 *M* OH^- aqueous pyridine of the dimer $[Mn_2TPP_2(H_2O)_2O]$ has now been briefly reported [111]. The dimer has a magnetic moment at 295°K of 4.12 B.M. The complex also shows a strong absorption at 867 cm^{-1} in the infrared which can be associated with an Mn–O–Mn stretch.

The zero field splitting of solid $[Mn(DMDepor)XH_2O]$ has been determined by the direct infrared method to be $\leqslant 3.5$ cm^{-1} for $X = Br^-$ and 9.25 cm^{-1} for $X = N_3^-$ (ref. 112).

ACKNOWLEDGMENTS

The author wishes to acknowledge the help of Mr. Joseph W. Klinehamer in obtaining some of the new data presented here. The author also expresses his gratitude to Prof. R.B. Jordan, Dr. R.E. Linder, Dr. J.R. Rowlands and Prof. A. Tulinsky for supplying their papers prior to publication.

Acknowledgment is made to the National Science Foundation for partial support of this research.

REFERENCES

1 J.E. Falk, *Porphyrins and Metalloporphyrins,* Elsevier, New York, 1964.
2 G.S. Marks, *Heme and Chlorophyll,* Van Nostrand, London, 1969.
3 B. Chance, R.W. Estabrook and T. Yonetani (Eds.), *Hemes and Hemoproteins,* Academic Press, New York, 1966.
4 L.J. Boucher, *J. Amer. Chem. Soc.*, 90 (1968) 6640.
5 J.H. Wang, *Accounts Chem. Res.*, 3 (1970) 90.
6 J.M. Olson, *Science,* 168 (1970) 438.
7 J. Zaleski, *Z. Physiol. Chem.*, 43 (1904) 11.
8 M. Calvin, *Rev. Pure Appl. Chem.*, 15 (1965) 1.
9 T.A. Zordan and L.G. Hepler, *Chem. Rev.*, 68 (1968) 737.
10 P.A. Loach and M. Calvin, *Biochemistry,* 2 (1963) 361.
11 A.D. Adler, F.R. Longo, F. Kampas and J. Kim, *J. Inorg. Nucl. Chem.*, 30 (1970) 2443.
12 J.H. Taylor, *J. Biol. Chem.*, 135 (1940) 569.
13 J.G. Montalvo and D.G. Davis, *Anal. Letters,* 1 (1968) 871.
14 D.A. Brisbin and R.J. Balahura, *Can. J. Chem.*, 46 (1968) 3431.
15 E.I. Choi and E.B. Fleischer, *Inorg. Chem.*, 2 (1963) 94.
16 D.K. Cabbiness and D.W. Margerum, *J. Amer. Chem. Soc.*, 92 (1970) 2151.
17 K. Kustin, R.F. Pasternak and E.M. Weinstock, *J. Amer. Chem. Soc.*, 88 (1966) 4610.
18 L.J. Boucher and J.W. Klinehamer, unpublished results.
19 L.J. Boucher and H.K. Garber, *Inorg. Chem.*, 9 (1970) 2644.
20 P. Hambright and E.B. Fleischer, *Inorg. Chem.*, 4 (1965) 912.
21 D.G. Davis and J.G. Montalvo, *Anal. Chem.*, 41 (1969) 1195.
22 L. Edwards, D.H. Dolphin and M. Gouterman, *J. Mol. Spectry.*, 35 (1970) 90.
23 R.S. Becker and J.B. Allison, *J. Phys. Chem.*, 67 (1963) 2662.
24 T. Yonetani and T. Asakura, *J. Biol. Chem.*, 244 (1969) 4580.

25 A. Yamamoto, L.K. Phillips and M. Calvin, *Inorg. Chem.*, 7 (1968) 847.
26 G. Engelsma, A. Yamamoto, E. Markham and M. Calvin, *J. Phys. Chem.*, 66 (1962) 2517.
27 P. Hambright, *Chem. Commun.*, (1967) 470.
28 E.B. Fleischer, *Accounts Chem. Res.*, 3 (1970) 105.
29 H.A.O. Hill, A.J. Macfarlane and R.J.P. Williams, *J. Chem. Soc., A*, (1969) 1704.
30 L. Rusnak and R.B. Jordan, *Inorg. Chem.*, in press.
31 E.B. Fleischer, S. Jacobs and L. Mestichelli, *J. Amer. Chem. Soc.*, 90 (1961) 2527.
32 C.B. Storm, A.H. Corwin, R.R. Arellano, M. Martz and R. Weintraub, *Inorg. Chem.*, in press. (1966) 2525.
33 J. Shack and W.M. Clark, *J. Biol. Chem.*, 198 (1962) 33.
34 L.J. Boucher, *J. Amer. Chem. Soc.*, 92 (1970) 2725.
35 J.L. Burmeister, *Coord. Chem. Rev.*, 3 (1968) 225.
36 S. McCoy and W.S. Caughey, *Biochemistry*, 9 (1970) 2387.
37 W.P. Hambright, A.N. Thorpe and C.C. Alexander, *J. Inorg. Nucl. Chem.*, 30 (1968) 3139.
38 F. Haurowitz, *Chem. Ber.*, 68 (1935) 1795.
39 R. Havemann, W. Haberditzl and K.H. Mader, *Z. Phys. Chem.*, 218 (1961) 71.
40 C. Maricondi, W. Swift and D.K. Straub, *J. Amer. Chem. Soc.*, 91 (1969) 5205.
41 P.L. Richards, W.S. Caughey, H. Eberspaecher, G. Feher and M. Malley, *J. Chem. Phys.*, 47 (1967) 1187.
42 R.M. Golding, P. Healy, P. Newman, E. Sinn, W.C. Tennant and A.H. White, *J. Chem. Phys.*, 52 (1970) 3105.
43 M. Gouterman, *J. Mol. Spectry*, 6 (1961) 138.
44 M. Zerner and M. Gouterman, *Theoret. Chim. Acta*, 4 (1966) 44.
45 M. Gouterman, *J. Chem. Phys.*, 30 (1959) 1139.
46 M.S. Fischer and C. Weiss, *J. Chem. Phys.*, 53 (1970) 3121.
47 L.J. Boucher, in S. Krischner (Ed.), *Coordination Chemistry*, Plenum Press, New York, 1969, p. 126.
48 W.S. Caughey, W.J. Fujimoto and B.P. Johnson, *Biochemistry*, 5 (1966) 3838.
49 D. Eastwood and M. Gouterman, *J. Mol. Spectry*, 35 (1970) 359.
50 L. Edwards, D.H. Dolphin, M. Gouterman and A.D. Adler, *J. Mol. Spectry*, 38 (1971) 16.
51 R.G. Pearson, *J. Chem. Educ.*, 45 (1968) 581, 643.
52 G.R. Seely and R.G. Jensen, *Spectrochim. Acta*, 21 (1965) 1835.
53 H. Kobayashi, M. Shimiza and I. Fujita, *Bull. Chem. Soc. Japan*, 43 (1970) 2335.
54 R.E. Linder and J.R. Rowlands, to be published.
55 M. Zerner and M. Gouterman, *Inorg. Chem.*, 5 (1966) 1699.
56 F.A. Cotton and G. Wilkinson, *Advanced Inorganic Chemistry*, 2nd edn., Wiley, New York, 1966, p. 728.
57 M. Zerner, M. Gouterman and H. Kobayashi, *Theoret. Chem. Acta*, 6 (1966) 363.
58 M. Gouterman, private communication.
59 E.W. Baker and J.R. Perumareddi, *Z. Naturforsch.*, 25b (1970) 911.
60 T.S. Davis, J.P. Fackler and M.J. Weeks, *Inorg. Chem.*, 7 (1968) 1994.
61 R. Dingle, *Acta Chem. Scand.*, 20 (1966) 33.
62 W.A. Eaton and R.M. Hochstrasser, *J. Chem. Phys.*, 49 (1968) 985.
63 W.A. Eaton and E. Charney, *J. Chem. Phys.*, 51 (1969) 4502.
64 B.M. Chen and A. Tulinsky, unpublished work;
B.M. Chen, *Ph. D. Thesis*, Michigan State University, 1970.
65 J.L. Hoard, G.H. Cohen and M.D. Glick, *J. Amer. Chem. Soc.*, 89 (1967) 1992.
66 E.J.W. Whittacker and R. Muntus, *Geochim. Cosmochim. Acta*, 34 (1970) 995.
67 A. Stone and E.B. Fleischer, *J. Amer. Chem. Soc.*, 90 (1968) 2735.
68 D.G. Davis and J.G. Montalvo, *Anal. Letters*, 1 (1968) 641.
69 G. Davies, *Coord. Chem. Rev.*, 4 (1969) 199.
70 D.A. Buckingham and A.M. Sargeson, in F.P. Dwyer and D.P. Mellor (Eds.), *Chelating Agents and Metal Chelates*, Academic Press, New York, 1969, p. 237.
71 N. Sutin, *Accounts Chem. Res.*, 1 (1968) 225.
72 M. Calvin, P.A. Loach and A. Yamamoto, in B. Jezouska-Trzebistowska (Ed.), *Theory and Structure of Complex Compounds*, Macmillan (Pergamon), New York, 1964, p. 13.

73 L.K. Phillips, *Ph. D. Thesis*, University of California, Berkeley, 1968.
74 A.W. Adamson, W.L. Waltz, E. Zinato, D.W. Watts, P.D. Fleischauer and R.D. Lundholm, *Chem. Rev.* 68 (1968) 541.
75 C.H. Kirksey, P. Hambright and C.B. Storm, *Inorg. Chem.*, 8 (1969) 2141.
76 R.H. Felton and H. Linschitz, *J. Amer. Chem. Soc.*, 88 (1966) 1113.
77 T. Yonetani, H.R. Drott, J.S. Leigh, G.H. Reed, M.R. Waterman and T. Asakura, *J. Biol. Chem.*, 245 (1970) 2998.
78 J.B. Allison and R.S. Becker, *J. Phys. Chem.*, 67 (1963) 2675.
79 R. Timkovich and A. Tulinsky, *J. Amer. Chem. Soc.*, 91 (1969) 4430.
80 P.A. Loach and M. Calvin, *Biochim. Biophys. Acta*, 79 (1964) 379.
81 A. Wolberg and J. Manassen, *J. Amer. Chem. Soc.*, 92 (1970) 2982.
82 T. Yonetani and T. Asakura, *J. Biol. Chem.*, 243 (1968) 3996.
83 T.L. Fabry, C. Simo and K. Javaherian, *Biochim. Biophys. Acta*, 160 (1968) 118.
84 J. Ozols and P. Strittmater, *J. Biol. Chem.*, 239 (1964) 1018.
85 M.R. Waterman and T. Yonetani, *J. Biol. Chem.*, 21 (1970) 5847.
86 D.C. Borg and G.C. Cotzias, *Nature*, 182 (1958) 1677.
87 M.S. Ashkinazi, T.S. Glickman and L.H. Zavgorodnyaya, *Dokl. Akad. Nauk SSR*, 170 (1966) 1195.
88 T.S. Glickman and O.V. Zabroda, *Biokhimiya*, 34 (1969) 302.
89 P.A. Loach and M. Calvin, *Nature*, 202 (1964) 345.
90 G.D. Dorough and F.M. Huenekens, *J. Amer. Chem. Soc.*, 74 (1952) 3974.
91 J.A. Elvidge and A.B.P. Lever, *Proc. Chem. Soc.*, (1959) 123, 195.
92 A.B.P. Lever, in H.J. Emeléus and A.G. Sharpe (Eds.), *Advances in Inorganic Chemistry and Radiochemistry*, Academic Press, New York, 1965, p. 27.
93 J.M. Robertson and J. Woodward, *J. Chem. Soc.*, (1940) 36.
94 C.G. Barraclough, R.L. Martin, J. Mitra and R.C. Sherwood, *J. Chem. Phys.*, 53 (1970) 1638.
95 P. Day, G. Scregg and R.J.P. Williams, *Biopolymers*. 1 (1964) 271.
96 J.H. Weber and D.H. Busch, *Inorg. Chem.*, 4 (1965) 469.
97 R. Taube and H. Munke, *Angew. Chem.*, 75 (1963) 639.
98 L.H. Vogt, A. Zalkin and D.H. Templeton, *Inorg. Chem.*, 6 (1967) 1725.
99 K. Fenkart and C.H. Brubaker, *J. Inorg. Nucl. Chem.*, 30 (1968) 3245.
100 H. Przywarska-Boniecka, in B. Jezouska-Trzesbistowska (Ed.), *Theory and Structure of Complex Compounds*, Macmillan (Pergamon), New York, 1964, p. 65.
101 R. Countryman, D.M. Collins and J.L. Hoard, *J. Amer. Chem. Soc.*, 91 (1969) 5166.
103 W.S. Caughey, H. Eberspaecher, W.H. Fuchsman, S. McCoy and J.O. Alben, *Ann. N.Y. Acad. Sci.*, 153 (1969) 722.
104 W.S. Caughey, *Bioinorg. Chem. Advan. in Chem.*, 100 (1971) 248.
105 J.G. Montalvo and D.G. Davis, *J. Electroanal. Chem.*, 23 (1969) 166.
106 D.G. Davis and R.F. Martin, *J. Amer. Chem. Soc.*, 88 (1966) 1316.
107 G. Lang, *Quart. Rev. Biophys.*, 3 (1970) 1.
108 E. Rabinowitch and Govindjee, *Photosynthesis*, Wiley, New York, 1969.
109 G.M. Cheniae, *Ann. Rev. Plant Physiol.*, 21 (1970) 2069.
110 G.A. Hamilton and A. Revesz, *J. Amer. Chem. Soc.*, 88 (1970) 2069.
111 E.B. Fleisher, J.M. Palmer, T.S. Srivastava and A. Chatterjee, *J. Amer. Chem. Soc.*, 93 (1971) 3162.
112 G.C. Brackett, P.L. Richards and W.S. Caughey, *J. Chem. Phys.*, 54 (1971) 4383.